INVESTIGATIONS IN ACHIEVING AND TAILORING NEGATIVE THERMAL EXPANSION IN CUZNAL AND TINB SHAPE MEMORY ALLOYS

A Thesis

by

XAVIER RENE HUERTA-SAN JUAN

Submitted to the Office of Graduate and Professional Studies of
Texas A&M University
in partial fulfillment of the requirements for the degree of

MASTER OF SCIENCE

Chair of Committee,	Ibrahim Karaman
Committee Members,	Hong Liang
	Raymundo Arroyave
Head of Department,	Andreas A. Polycarpou

December 2018

Major Subject: Mechanical Engineering

ABSTRACT

Thermal Expansion is a material property that must be accounted for when designing objects where the operating temperature is larger or smaller than the ambient temperature, i.e. cryogenic tanks, and in precision instruments such as lasers, optical instruments. Currently, metals used in such applications have positive coefficients of thermal expansion. When the instruments become operational, the metals used will contract if cooled or expand when heated, causing critical distances, such as focal lengths in optics and lasers, to change, and fasteners to loosen. Having a metal that with a negative coefficient of thermal expansion can give designers a way to improve these instruments. Research in investigating inexpensive methods of producing negative thermal expansion in metals was conducted. Two different compositions of Copper Zinc Aluminum Shape Memory Alloy were investigated to see if applying known methods of producing negative thermal expansion in shape memory alloys would produce the same effect. Titanium Niobium is known to have negative thermal expansion properties. Different cold processing methods were investigated to see the effects in the coefficient of thermal expansion. Two different methods of tailoring the thermal expansion coefficient were investigated as well: welding TiNb to Ti , and post heat treating TiNb after having a negative coefficient of thermal expansion. CuZnAl showed that the coefficient of thermal expansion can be lowered, but it would remain positive. The different methods of processing TiNb all showed to produce negative coefficients of thermal expansion in TiNb to different degrees. Joining TiNb to Ti by welding produces a coefficient of thermal

expansion that is between that of TiNb and Ti. Post heat treating TiNb showed that the coefficient of thermal expansion can be altered by controlling the temperature and time of the heat treatment. The two compositions of CuZnAl cannot be used in applications needing negative thermal expansion. TiNb has multiple method of having negative thermal expansion produced and multiple ways of tailoring the thermal expansion properties, making it an optimal material for application.

DEDICATION

I would like to dedicate this Thesis and the work that I do to my family, friends, and all those who have mentored and guided me through my graduate studies.

ACKNOWLEDGEMENTS

I would like to thank my committee chair Dr. Karaman and my friend and mentor Dr. Monroe. I would also like to thank my committee members, Dr. Hong Liang and Dr. Arroyave for their guidance and patience.

To all the friend I have made and all the friends that have supported me, thank you for your support.

Finally, I would like to thank my parents for sacrificing for me, pushing, and encouraging me to continue my education.

CONTRIBUTORS AND FUNDING SOURCES

Contributors

This work was supervised by a thesis committee consisting of Professor Ibrahim Karaman, Professor Raymundo Arroyave of the Department of Material Science and Engineering, and Professor Hong Liang of the Department of Mechanical Engineering.

Funding Sources

NSF SPIR Award Number 1632571

Project Title: Zero Thermal Expansion Alloys for Lasers

TABLE OF CONTENTS

Page

LIST OF FIGURES

Page

LIST OF TABLES

Page

1. INTRODUCTION

Shape memory alloys (SMA) are alloys that show the shape memory effect, an effect where an alloy remembers its shape before deformation and returns to its shape through martensitic transformation. These alloys undergo martensitic phase transformations because of applied thermomechanical loads and can recover permanent strains when heated above a certain temperature[i]. At high temperature, the crystal lattice is in a high symmetry, usually cubic[ii], parent austenite phase. At low temperature, the crystal lattice is at a lower symmetry phase called martensite. Martensitic transformation is a diffusionless phase transformation driven by the nucleation and growth of the martensite phase, where the atoms move cooperatively, and by a shear-like mechanism[iii], from the parent austenitic phase. A simplified model of phase transformation is shown in Figure 1. The high-symmetry, cubic, austenitic phase transforms into the lower symmetry martensite by the atoms displacing in an ordered fashion. In Figure 1, there are two martensite lattices, A and B, they are both the same structure, but have different orientations; this is because martensite is a lower symmetry phase, and can form many different variants from its parent phase[iv]. When heated, the martensite will revert to its parent phase in the original orientation. Martensitic transformation can be induced both thermally and through applied stress[v].

Martensitic transformation occurs over a range of temperatures. The transformation temperature that occurs while transforming from austenite to martensite that occurs while cooling is called the martensite start temperature, M_s. When the transformation from

austenite to martensite finishes, the temperature reaches the martensitic finish temperature, M_f. When heating, the temperature at which martensitic begins to transform to austenite is called the austenite start temperature, A_s. When the transformation finishes, the temperature will be at the austenite finish temperature, A_f.

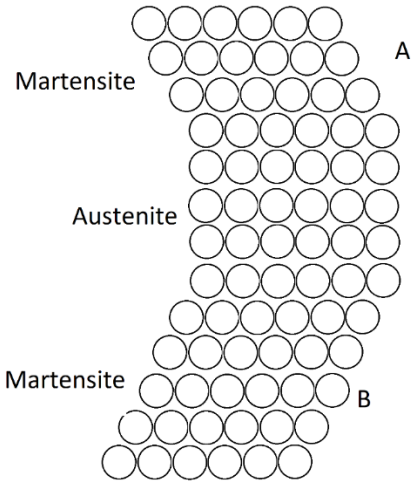

Figure 1-Simplified Model of Austenite and Martensite Phase and Variants.

Thermal expansion occurs in all materials. In metals thermal expansion is caused by the changed in distance between the atoms as they vibrate; when energy in the form of heat is added into the material, the average atomic distance increases. When energy is lost, the average distance between atoms decrease. Commonly used metals exhibit positive thermal expansion, or PTE, meaning that the material expands as it is heated and contracts as it is cooled.

Negative Thermal Expansion (NTE) can be seen in ceramics and in metals. FeNi-based Invar alloys has shown very low thermal expansion, very close to 0, making it useful in applications where thermal expansion affects system design. Ceramics have limited use in their applications because of their low fracture toughness, and low thermal conductivity. Although Invar's CTE and mechanical properties are useful in application, it has a limited scope of use since the lowest CTE it can reach is near zero.

Currently, the only way to alter the coefficient of thermal expansion (CTE) of both ceramics and Invar is by changing their chemical composition. Recently, it has been shown that martensitic alloys have NTE at the atomic level. By using thermo-mechanical processing methods, the CTE of martensitic alloys can be tailored between positive and negative values by crystallographically texturing the martensite. Previous methods used to texture the martensite were cold rolling and incremental tension test while the alloys were in martensite phase. It was shown that a relationship between the austenite and martensite lattice parameters and the positive and negative CTE values exist. The crystallographic NTE directions correspond to the crystallographic directions that were smaller in austenite than martensite and the crystallographic PTE directions correspond to the crystallographic directions where austenite is larger than martensite. This clearly shows a relationship between the PTE and NTE with the austenite and martensite lattice parameters. Inverse pole figures showed that the macroscopic CTE responses are achieved by reorienting the martensite variants along the sample using thermo-mechanical processing methods. After TiNb was 50% cold rolled, the plane direction that exhibited

the most NTE at the atomic level exhibited strong texture along the rolling direction and a macroscopic NTE could then be observed.

By re-orienting the martensite, macroscopic NTE in shape memory alloys could be observed. This is extremely useful in applications that require thermal expansion compensations due to thermal gradients, such as optical systems in lasers and powerful satellite telescopes. Currently, TiNb is the most useful SMA that is being manufactured because of its broad range of PTE and NTE as well as its high malleability compared to other SMAs that have been studied. For SMAs to become more useful in applications, different ways of processing them to have NTE must be discovered. Since it is known that by reorienting the martensite variants results in NTE, macroscopic NTE can be produced by any method were the martensite is re-oriented. The significance of finding out different methods of re-orienting the martensite can result in producing SMAs with different shapes and with different negative CTEs that can be used in different applications. One goal in this research project is to find multiple ways of producing TiNb that has negative CTE. To do this, $Ti_{22}Nb_{78}$ was processed in five ways: forging, rolling, forward extrusion, backward extrusion, and tube drawing. Although the CTE of TiNb can be tailored by increasing the deformation percentage, the relationship between rolling deformation and macroscopic CTE response is not linear, making precise CTE tailoring difficult to reproduce. Another goal was to further improve the applicability of TiNb by finding out ways to precisely tailor the CTE. Since texturing is one of the causes of NTE, a heat treatment study was conducted to see if the NTE coefficient could be precisely tailored

using different temperatures and times to control the amount of texture relaxation. When used as a structural component, TiNb will have to be joined to another material. Materials can be joined together in various ways, whether it be mechanical or chemical, the greatest effect joining would have on a SMA with NTE is if the joining process heated the materials above its martensitic transformation temperature. For this study, mechanical properties as well as the CTE change of TiNb welded to itself and another piece of Titanium was investigated. Using laser welding, the CTE of TiNb-Ti sample was investigated to see if the CTE can be tailored using CTE compensational methods and what effects welding had on the CTE of TiNb.

Previously, SMAs studied that exhibit NTE were NiTiPd, CoNiGa, and TiNb. For applicational use, TiNb is the best choice because it exhibited one of the largest NTE and it had the greatest malleability compared to the other SMAs studied, making it easier to process. More research into other SMAs is needed to expand the use of SMAs with NTE properties. CuZnAl is an optimal SMA to investigate for NTE. The goal for CuZnAl SMA is to find out if it is possible to achieve NTE coefficients. CuZnAl is optimal because it is relatively inexpensive, more malleable than previous SMAs with NTE, and has a high thermal conductivity.

Several steps must be accomplished to see if CuZnAl has tailorable NTE:

1. Because there is an apparent relationship between parent austenite and martensite phases corresponding to PTE and NTE values, a homogenous martensitic microstructure must be achieved.
2. To have NTE, NTE must be observed at the atomic level. Using X-ray diffraction, the lattice parameter of martensite responses to increasing temperature can be seen using X-Ray Diffraction(XRD).
3. The macroscopic response to thermo-mechanical deformation must be checked to see if reorientation of martensite variants occurs and if CTE changes with reorientation.

CuZnAl is unlike other SMA's because of the multiple martensitic phases that can occur. Because 6 different martensite variants can occur, a heat treatment study needs to be conducted to see the effects of heat treatments to the microstructure.

SMAs with NTE coefficients have many practical uses as well. As the temperature in lasers and optical systems changes, the materials that are in the systems will expand or contract; because most systems are made with metallic parts, the change in focal length is difficult to compensate. Laser and optical systems can benefit from the NTE of SMAs by having better control of the focal lengths in lenses. SMAs can also be used to better design cryogenic systems by giving engineers another property they can manipulate.

2. INVESTIGATIONS INTO CUZNAL

2.1. Materials and Methods

2.1.1. Microstructural Heat Treatment Study

Two different CuZnAl alloys, $Cu_{75}Zn_{18}Al_7$ and $Cu_{68}Zn_{25}Al_7$ (at.%), were casted in rectangular bar. Square plates samples were cut using a band saw. The samples were cold rolled at room temperature and turned ninety degrees after each pass. The distance between the rollers was incrementally decrease by 0.005" after each pass until the samples height were 50% reduced.

Rolled samples of both compositions were electro-discharged machined into 12mmx12mm square samples with a thickness of 4 mm. Homogenizing heat treatments were performed on both compositions for various times and temperatures. The heat treatment specifications for both compositions are shown in Table 1 and Table 2.

Table 1 Heat Treatment Specifications for $Cu_{75}Zn_{18}Al_7$

Time	Temperature(°C)
As Cast	As Cast
20 minutes	800
20 minutes	900
20 minutes	850
20 minutes	630

Table 2 Heat Treatment specifications for $Cu_{68}Zn_{25}Al_7$

Time	Temperature(°C)
As Cast	As Cast
6 hours	850
6 hours	900
6 hours	929
6 hours	941
6 hours	935
6 hours	935
3 hours	935
3 hours	850
3 hours	900
20 minutes	700
20 minutes	750
20 minutes	650
20 minutes	900
20 minutes	850
20 minutes	630
20 minutes	935
20 minutes	800

Rolled samples of $Cu_{68}Zn_{25}Al_7$ were also electro-discharged machined into strip that were 38mm long, 7mm wide, and at varying thickness: 1mm, 0.75mm, and 0.5mm. Homogenizing heat treatments were performed at 920ºC for 20 minutes.

All heat treated samples were etched using an etching solution consisting of 5g of Fe_3Cl, 12.5 ml HCl, and 50 ml distilled water. The samples were placed in the etchant for

approximately 4 seconds then placed in distilled water. The microstructures of the samples were examined under an optical microscope.

2.1.2. Isobaric Tension Test

Tension dog samples measuring 25mm long with a gauge length of 8mm were electro-discharged machined from the samples with thicknesses of 1mm, 0.75mm, and 0.5mm and the heat treatments stated earlier. Monotonic tensile tests were conducted using a servo-hydraulic MTS loaded with an Interface load cell with a capacity of 2500 lbf. The monotonic tension tests were conducted at a 0.004 in/s strain rate until failure. Stress and strain were continuously recorded using a strain gauge.

Isobaric heating and cooling test were also performed on 1mm thick samples using the same strain gauge and MTS machine. The samples were wrapped in insulation and iteratively strained, cooled, and heated in between each strain step. The isobaric heating and cooling test strained at 0.05%, 1.0%,1.5%,2.0%, 3.0%, 5.0%, 8.0%,10.0%, and 12.0%. In between each strain step, the samples were cooled to -50ºC and heated to 100ºC while the strain was continuously recorded.

2.1.3. Measuring Transformation Temperatures

Differential scanning calorimetry (DSC) was used to determine the martensite to austenite phase transformation temperature of both compositions with different homogenizing heat treatments based on microscopy. The cooling and heating rate was set to 10ºC a minute.

2.1.4. X-Ray Diffraction Testing

X-Ray Diffraction (XRD) was done on a Bruker attached with a Cu. XRD was performed on both compositions that were homogenized at different temperatures shown in Table 3 and Table 4 . The selected homogenizing temperature for $Cu_{68}Zn_{25}Al_7$ was 925°C for different length of time. Samples of $Cu_{68}Zn_{25}Al_7$ after being homogenized were heated on the Bruker XRD machine using a platinum strip at different temperatures. XRD was performed at temperatures ranging from 30°C to 100°C in intervals of 10°C to compare changed in distances between planes as temperature increases.

Table 3 **Homogenizing Heat Treatments of $Cu_{75}Zn_{18}A_7$**

Time(hours)	Temperature(^oC)	Atmosphere	Quench
0.25	950	Air	Water (23^oC)
0.5	975	Air	Water (23^oC)
3	975	Air	Water (23^oC)
3	950	Air	Water (23^oC)
3	800	Air	Water (23^oC)
5	975	Air	Water (23^oC)
7	950	Air	Water (23^oC)

Table 4 **Homogenizing Heat Treatments of $Cu_{68}Zn_{25}Al_7$**

Time(hours)	Temperature(^oC)	Atmosphere	Quench
6	935	Air	Water (23^oC)
3	915	Air	Water (23^oC)
3	900	Air	Water (23^oC)
3	800	Air	Water (23^oC)
0.25	925	Air	Water (23^oC)
3	925	Air	Water (23^oC)
3	925	Air	Water (23^oC)
3	925	Air	Water (23^oC)
6	935	Air	Water (23^oC)

2.2. Results and Discussion

2.2.1. Study on $Cu_{68}Zn_{25}Al_7$

2.2.1.1. Microstructural Study

Microstructural changes resulting from different heat treatments were studied to determine the homogenizing heat treatment that resulted in the most uniform martensitic microstructure.

Figure 2 shows the optical microscopy for $Cu_{68}Zn_{25}Al_7$ .Based on the optical microscopy, there exist a dual phase microstructure in the as-cast form of $Cu_{68}Zn_{25}Al_7$.

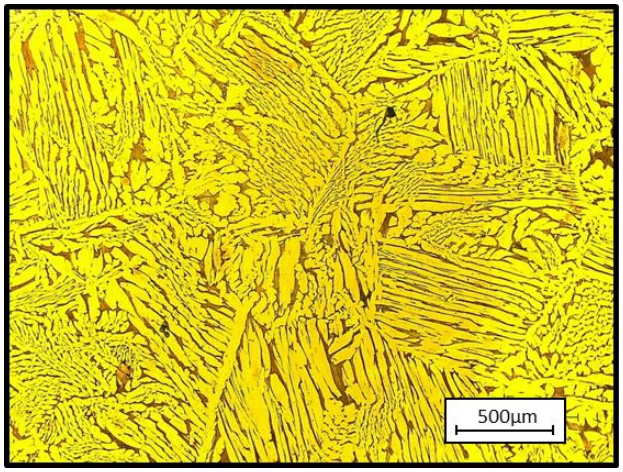

Figure 2 - Optical Microscopy for As Cast Samples of $Cu_{68}Zn_{25}Al_7$

Multiple studies in Cu-based SMAs suggested heat treatments between 800ºC to 850ºC for at most 30 minutes. This was attempted but the resulting microstructures were not repeatable and continued having the dual phase similar to the one shown in Figure 2. A heat treatment experiment was designed to see the effects of temperature on $Cu_{68}Zn_{25}Al_7$. The purpose of this heat treatment was to find the temperature where B2 austenite exist, since B2 ordered austenite is the parent phase that martensite reverses back into. Another crucial factor to consider is the quenching rate. $L2_1$ is an intermediate phase that exist between the high temperature parent austenite and martensite phase. Since $L2_1$ ordered austenite can be suppressed if the quenching rate is fast enough, the quenching medium must be considered. Since the temperature difference between the high temperature B2 phase and room temperature is large, room temperature water was used as the quenching medium.

Heat treatments were conducted at discrete temperatures for 20 minutes, shown in Figure 3. A magnified view detailing an apparent change in microstructure is shown in Figure 4. The dual phase present in the as cast form is repeatedly shown for temperatures below 800ºC. At 850ºC, there seems to be a transformation at the darker phase present temperatures below 800ºC. The darker phase grows at the expense of the lighter phase and martensite begins to appear. At 900ºC there is a drastic change in microstructure, the dual phase previously seen is no longer present. Grains of martensite begin to develop. The martensite grains are very large, some measuring over 1mm in width. At 935ºC there is a similar microstructure, where martensite and large grains are present, but the martensite is no longer lamellar but is more needle shaped. At both 900ºC and 935ºC, there are some precipitates at the grain boundaries.

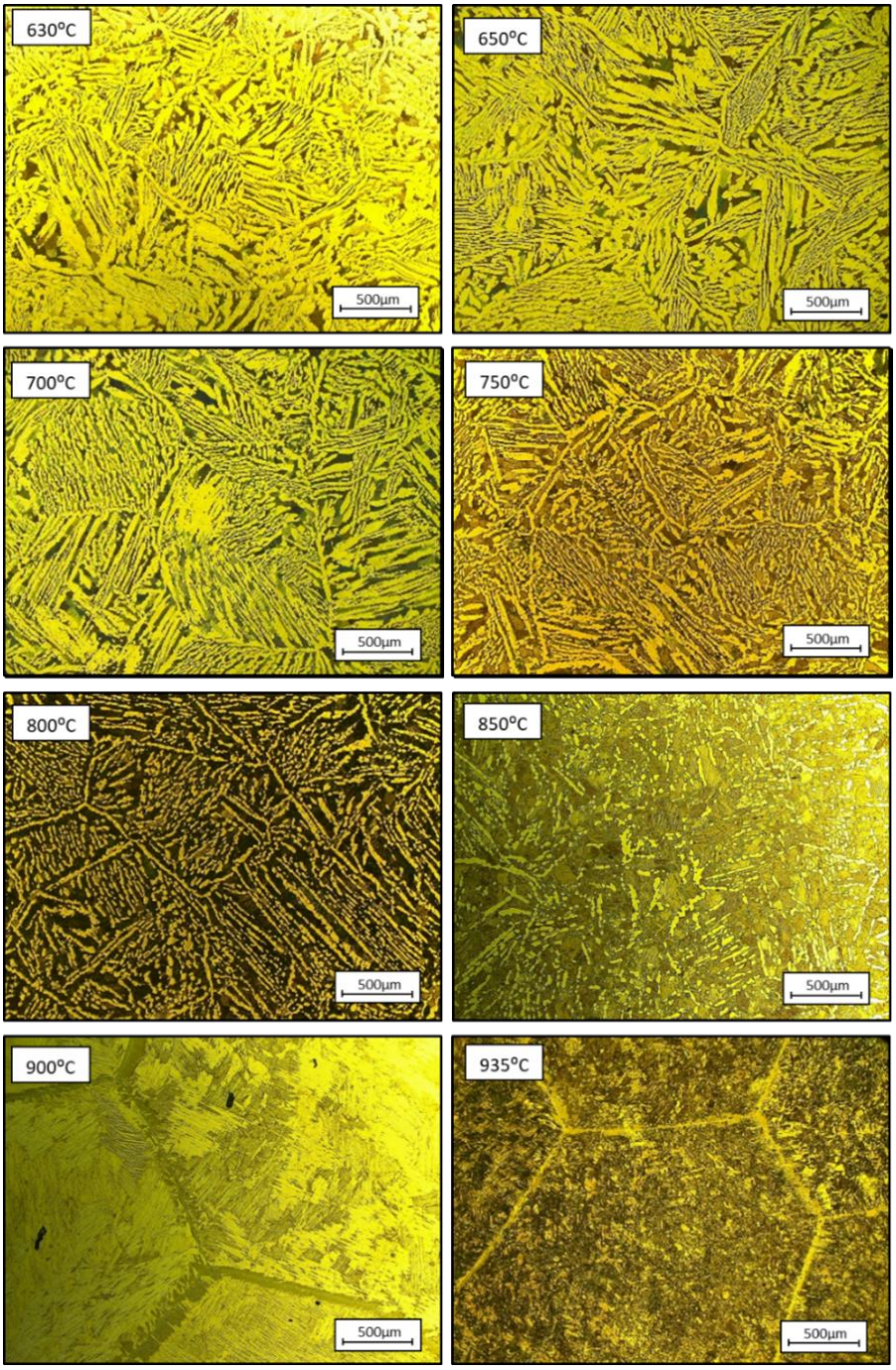

Figure 3 - Heat Treatment Results of $Cu_{68}Zn_{25}Al_7$ Heat treated for 20 Minutes at Discrete Temperatures.

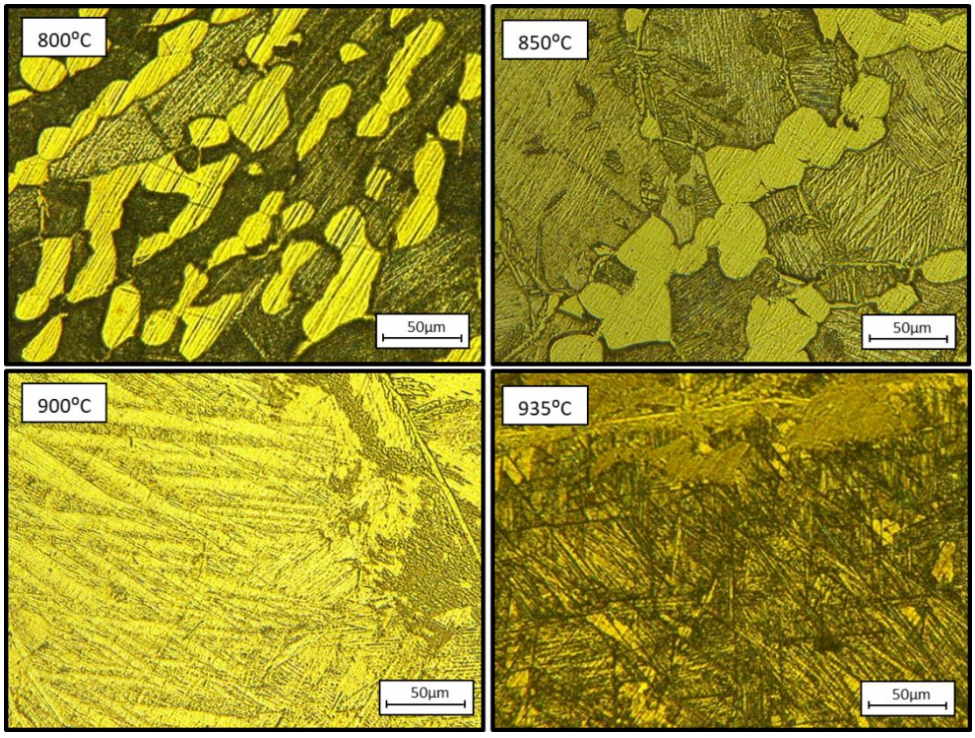

Figure 4 - Magnification of Heat Treatment Results of $Cu_{68}Zn_{25}Al_7$ Between 800ºC and 935ºC

Based on the microstructural results and the phases present in CuZnAl SMAs, it is believed that the dual phases present are composed of B2 and $L2_1$ austenite. At temperatures above 900ºC, B2 austenite exist, causing the microstructure after quenching to be mostly austenite. At temperature below 900ºC, both phase are present, resulting in a dual phase microstructure after quenching. The heat treatment study showed that $Cu_{68}Zn_{25}Al_7$ must be heat treated above 935ºC for at least 20 minutes. The cause of different variants of martensite present at 900ºC and 935ºC is unknown and the presence of precipitates at the grain boundaries must be eliminated, as precipitates might cause a

problem when attempting to re-orient the martensite. Because $L2_1$ austenite can be suppressed if the sample is quenched fast enough, a high temperature heat treatment study was conducted to find the highest temperature $Cu_{68}Zn_{25}Al_7$ could be heated to. Suppressing $L2_1$ can eliminate the precipitates at the grain boundaries. $Cu_{68}Zn_{25}Al_7$ were heat treated at 929ºC ,935ºC, and 941ºC for 20 minutes and quenched in water. Figure 5 shows the results of the high temperature heat treatment study. All heat treatments resulted in comparable sized grains and martensites. At 935ºC, there was lamellar martensite present, which is different than the needle like martensite that was present at a different heat treatment with the same settings. At 929ºC, there is needle like martensite. At both 929ºC and 935ºC, there are precipitates at the grain boundaries, but at the higher temperature, the precipitates are less pronounced. At 941ºC, the sample begins to melt, losing its shape and creating pockets of melted sections. Discovering the melting temperature of this composition is useful because it put provides the highest temperature $Cu_{68}Zn_{25}Al_7$ can be heat treated at. With this information, $Cu_{68}Zn_{25}Al_7$ can be heat treated past the $L2_1$ phase, making it easier to have the most martensite possible. The reason different variants of martensite that appear with similar heat treatments is unknown. A heat treatment that can give less sample variance would be ideal for future experiments.

In addition to the effects of temperature, the effects of time were also investigated. Since the temperature ranges for different phases are known, two temperatures were investigated to see what how the length of the heat treatment affects the microstructure. The

temperature before the phase change occurs, 850ºC, and the highest temperature that the sample can be heated to before melting, 935º were investigate. The results are shown in Figure 6. Different samples were heat treated for 20 minutes, 3 hours, and 6 hours at 850ºC and 935ºC. For both samples, the microstructure remains unchanged. For the samples heat treated at 850ºC, grain size remains the same and the dual phase microstructure is present for all times.

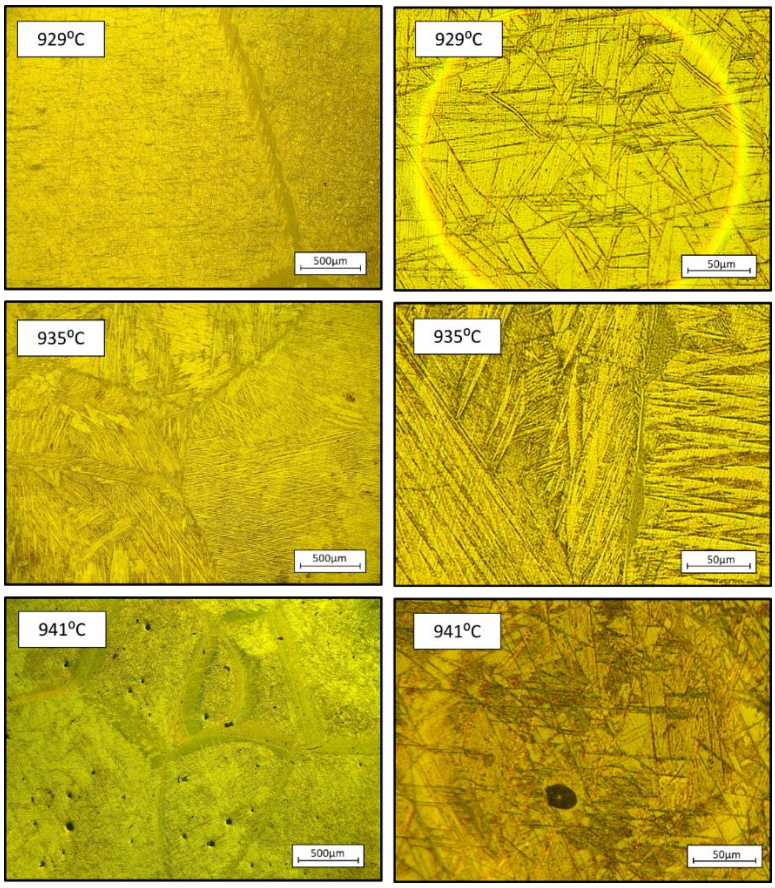

Figure 5 - High Temperature Heat Treatment Study of $Cu_{68}Zn_{25}Al_7$

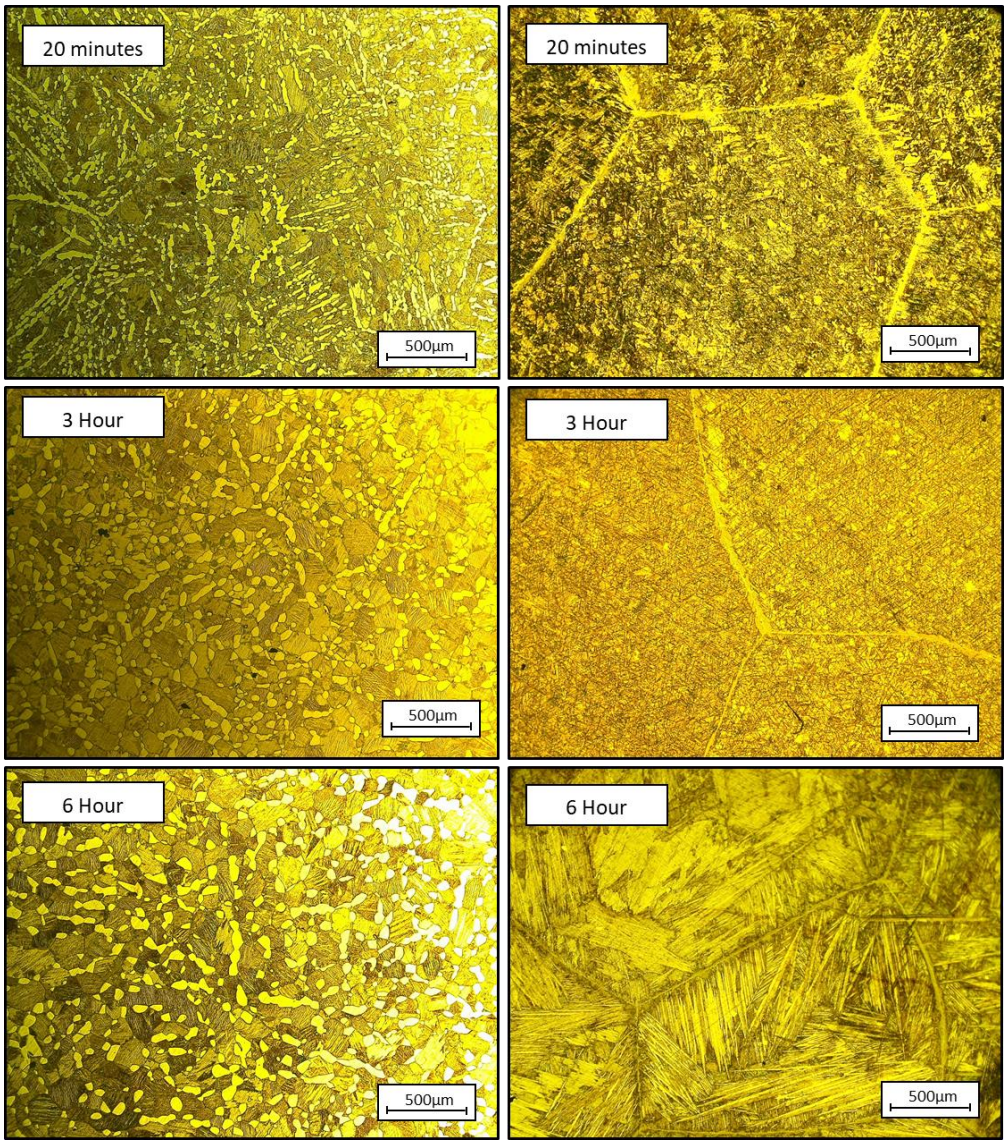

Figure 6 - Microstructure of $Cu_{68}Zn_{25}Al_7$ After Heat Treated at 850⁰ (left) and 935ºC (right) For Different Lengths of Time.

Samples heat treated at 935ºC have the same grain size and precipitates at the grain boundaries for all times. Martensite is present for all times, but the martensite varies

between needle like and lamellar between samples. This also happens between samples when temperatures changes. The reason for different martensites is unknown but does not seem to be dependent on temperature or length of the heat treatment.

2.2.1.2. X-Ray Diffraction Study on $Cu_{68}Zn_{25}Al_7$

The heat treatment study resulted in showing that $Cu_{68}Zn_{25}Al_7$ has sample to sample variation between similar heat treatments. The homogenizing temperature should be above 900ºC and the length of the heat treatment has no effect on the microstructure. With this information, XRD can be performed to see the effect of temperature on the planar spacing. If the XRD peaks shift to the right when the sample is heated, then the planar spacing is decreasing when heated, meaning that NTE is present. To determine the highest temperature the sample can be heated to before transforming to austenite, DSC was used. The DSC result is show in Figure 7. There is no distinct change between phases, but there is a slight curve between 220ºC and 320ºC. For this study, it was decided the A_s temperature would be 220ºC. Once the upper temperature was decided, different microstructures were investigated using XRD. Two separate heat treatments were investigated using XRD. One sample was heat treated at 800ºC for 3 hours and quenched in room temperature water. The results shown in Figure 8 are XRD scans of a sample heat treated at 800°C, taken at increasing temperatures. All the peaks shift to the left, indicating that there is no negative CTE at the atomic level. There are a few phase transformations, shown at 89º and 46º. This heat treatment produces a dual phase microstructure.

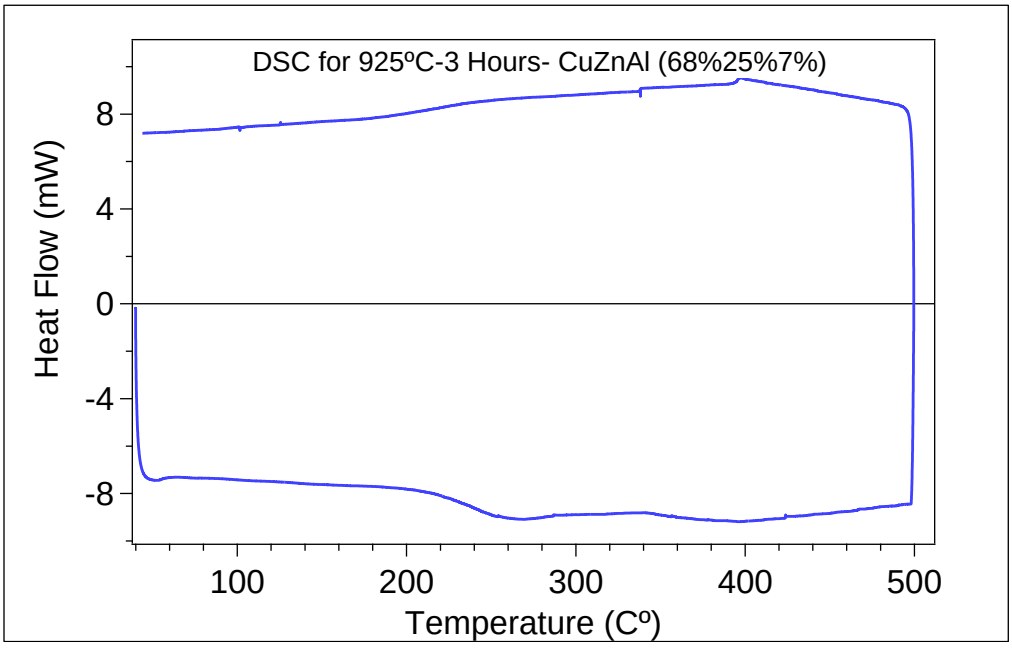

Figure 7 - DSC Result of $Cu_{68}Zn_{25}Al_7$ Heat Treated at 925ºC for 3 Hours

There seems to be a meta-stable martensite that transforms to austenite at transformation temperatures lower than what the DSC analysis shows. The sharp peaks at 190ºC are indicative of austenite phases and the broader peaks at lower temperatures are martensite peaks. The previous heat treatment study suggested the dual phase to be multiple phases of austenite, but XRD shows that is a meta-stable martensite and an austenite phase.

Another sample of $Cu_{68}Zn_{25}Al_7$ that was heat treated at 925ºC for 15 minutes and quenched in room temperature water was analyzed using several scans of XRD at

incremental temperatures. This heat treatment produced a martensite phase with precipitates at the grain boundaries. There were no right shifts as the temperature of the XRD scan was increased, thus showing that there is no NTE at the atomic level. At temperatures above 180ºC, martensite peaks transform into austenite peaks. This transformation agrees with the DSC data of the transformation temperature occurring around 230ºC. A second incremental temperature XRD scan was performed on the same sample. The result is shown on the bottom of Figure 9. There are no martensite peaks, even at room temperature. As the temperature increases, there is no right shifts. The results of the second scan show that $Cu_{68}Zn_{25}Al_7$ may not be a two way SMA.

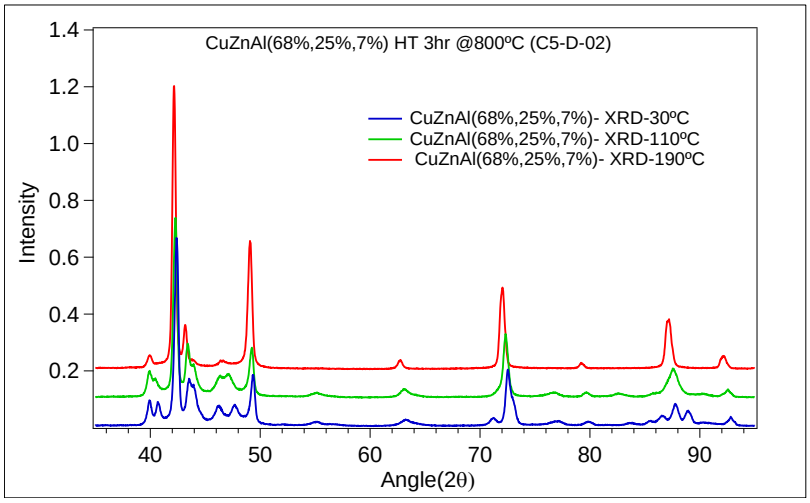

Figure 8-XRD of $Cu_{68}Zn_{25}Al_7$ Heat Treated for 3 Hours at 800C

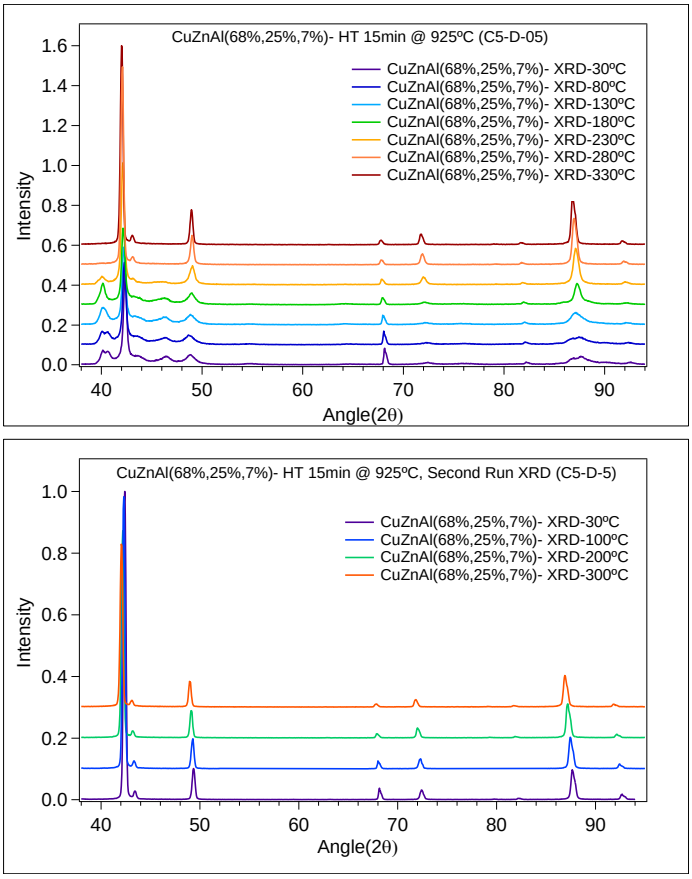

Figure 9- Incremental Heated XRD of $Cu_{68}Zn_{25}Al_7$ Heat Treated at 925º for 15 minutes, (Top) first XRD run, (Bottom) Second XRD Run

Although it may not be a two way SMA, the relationship between NTE and crystallographic phases does not depend on the SMA being a two way SMA. The peaks of the XRD results could not be indexed, as the several types of martensites and austenites all show similar peaks, making it very difficult to index. Indexing would have provided more information, but the change in planar distance is what was most important to

determine if NTE was possible. The XRD results of both $Cu_{68}Zn_{25}Al_7$ samples showed that there is no NTE at the atomic level. Although previous studies showed that SMAs with NTE had NTE at the atomic level, $Cu_{68}Zn_{25}Al_7$ may still have tailorable CTE. To test if tailorable CTE is possible, more heat treatment studies must be conducted to have less sample to sample variation. The previous heat treatment study showed that temperature affected the microstructure of the samples and the amount of time the heat treatment lasted had no effect on the microstructure. Heat treatments above 900ºC produced large martensite grains. Sample to sample variation was still occurring even though samples were heat treated at the same conditions. Figure 10 shows an example of sample to sample variation. Two samples were heat treated, separately, ay 925ºC for 3 hours. Both samples have different sets of peaks. Another sample was heat treated for the same amount of time at 915ºC and has a different set of peaks.

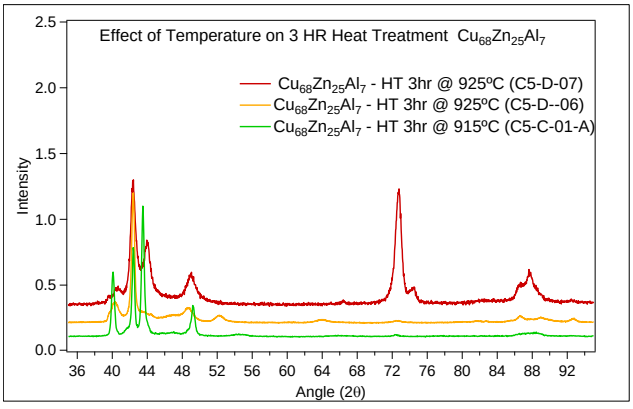

Figure 10 - XRD Results of $Cu_{68}Zn_{25}Al_7$ Heat Treated at Different Temperatures above 900º

2.2.1.3. Quenching Study and Mechanical Testing on $Cu_{68}Zn_{25}Al_7$

Since previous experiments only tested for temperature and time, quenching rate was chosen as a third factor that may affect the microstructure. Increasing the quenching rate can completely suppress the $L2_1$ austenite phase and allow the B2 austenite to completely transform to martensite. Previously, it was thought that the temperature difference between the homogenizing temperature and the water quench, in addition to the high thermal conductivity of CuZnAl, would be enough to suppress the $L2_1$ austenite phase, but the sample to sample variation has shown otherwise. There are multiple ways to increase the quenching rate. Below are three different ways the quenching rate was increased.

1. Increase the temperature difference of the heated sample and the quench medium. The water temperature was decreased from room temperature to an ice bath.
2. Increase the efficiency of the quench by reducing bubble formation and increasing surface contact. Salt was added to the water, along with ice, to make an ice brine.
3. Reduce the heat capacity of the sample. The sample thickness was decreased.

2.2.1.3.1. Ice Water Quench

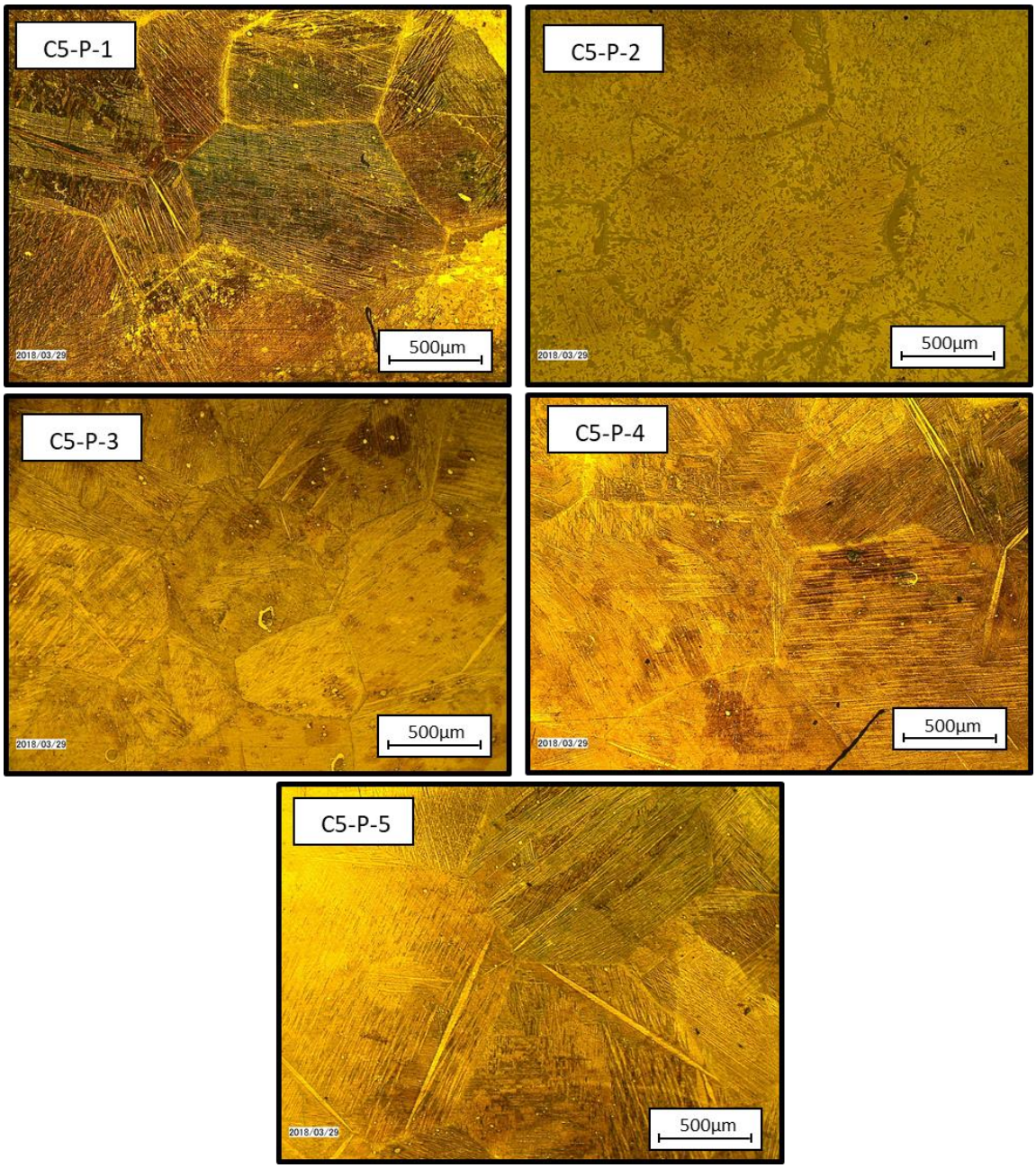

Figure 11- Different samples of $Cu_{68}Zn_{25}Al_7$ Heat Treated at 920ºC for 30 Minutes and Quenched in Ice Water

Because the heat treatment study showed that temperatures above 900ºC resulted in a microstructure with large martensitic grains, the temperature for the heat treatment studies performed were chosen to be 920ºC. Figure 11 shows the microstructure of five different samples of $Cu_{68}Zn_{25}Al_7$ heat treated at 920ºC for 30 minutes, these samples were all 1mm thick. The samples were heat treated separately and all were quenched in and ice water bath. The resulting microstructures were very similar to the microstructures of the previous heat treatment study, shown in Figure 3. The have large martensitic grains. The biggest difference between the quenching in room temperature water and quenching in an ice bath is that the lamellar martensite is consistent between samples. The only sample that looks different is C5-P-2. Another major difference is the reduction of precipitates at the grain boundaries. The two differences between this heat treatment and the one shown in Figure 3 is the temperature of the quenching medium and the sample thickness, previous samples had a sample thickness of 3mm. The sample to sample variation decreased based off optical microscopy.

Since martensite reorientation needs to occur to tailor the CTE, isobaric tension tests were performed to determine if martensite reorientation occurs in the sample and the range of the martensite reorientation. Figure 12 shows the results of four of the five samples shown in Figure 11. Although 3 of the 4 samples look similar, their isothermal thermal tension results are different. C5-P-1 had the most martensitic reorientation, yielding at 125MPa. C5-P-2 had the largest yield strength and ultimate tensile strength. C5-P-2 is also the

sample with the least similarity between other samples. The samples microstructures look very similar, but their mechanical properties vary. C5-P-5 was chosen to do an incremental strain tension test. The sample was strained to a preset percentage, the temperature of the sample was decreased to -65ºC and heated to 100ºC. This step was repeated at higher strains. The CTE was then calculated using the thermal strain between temperature changes. C5-P-5 was expected to mechanically behave like the samples with similar microstructures. After the incremental strain test was completed, the resulting stress vs. strain curve was compared to the other samples isothermal tension test to see which sample C5-P-5 behaved like the most.

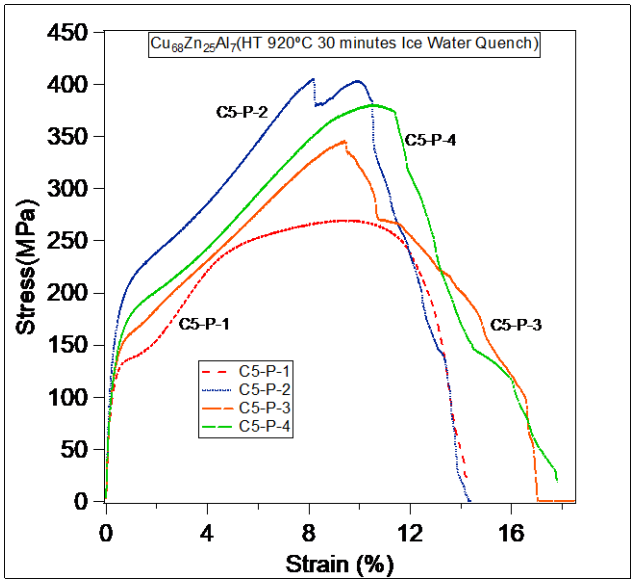

Figure 12 - Monotonic Tension Test of Samples Heat Treated at 920°C for 30 Minutes and Quenched in Ice Water

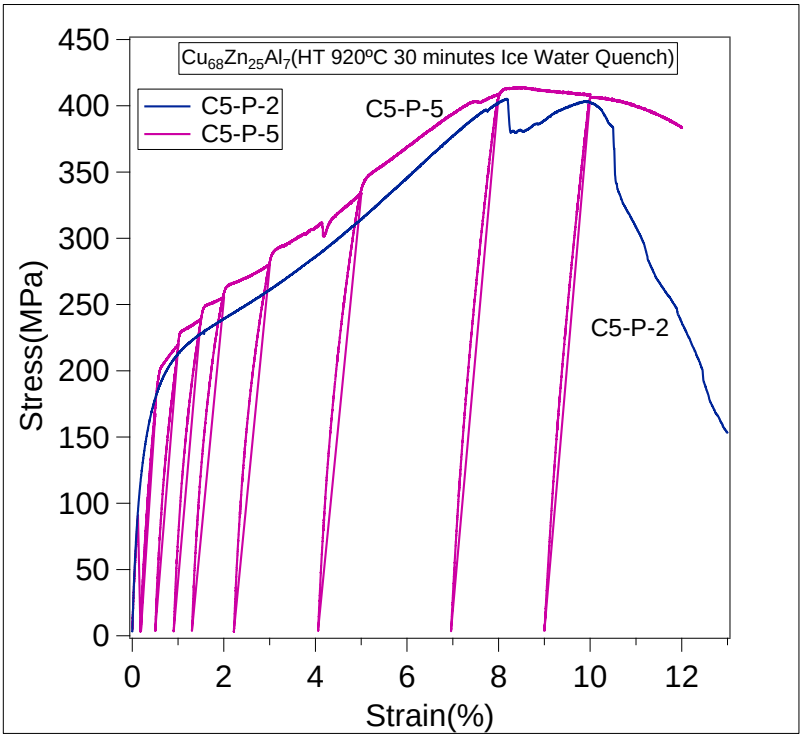

Figure 13 – Comparison of Isobaric Heating and Cooling Tension Results and a Monotonic Tension Test.

The sample comparison is shown in Figure 13. The CTE was calculated, shown in Figure 14.. The highest CTE change occurred while heating, dropping from 17.9 ppm to 14.8 ppm The CTE dropped as the sample was strained until the UTS was reached, where the CTE increased. C5-P-2 was not expected to share the mechanical behavior of C5-P-2 because of the macroscopic differences. This shows that sample to sample variation still occurs even when the samples show similar macroscopic characteristics. The CTE dropped almost linearly as the strained increase, showing that CTE can be tailored to an

extent. During martensite reorientation, CTE can be decreased. It is possible that upon larger martensite reorientation, similar to C5-P-1, the CTE can be dropped to lower values.

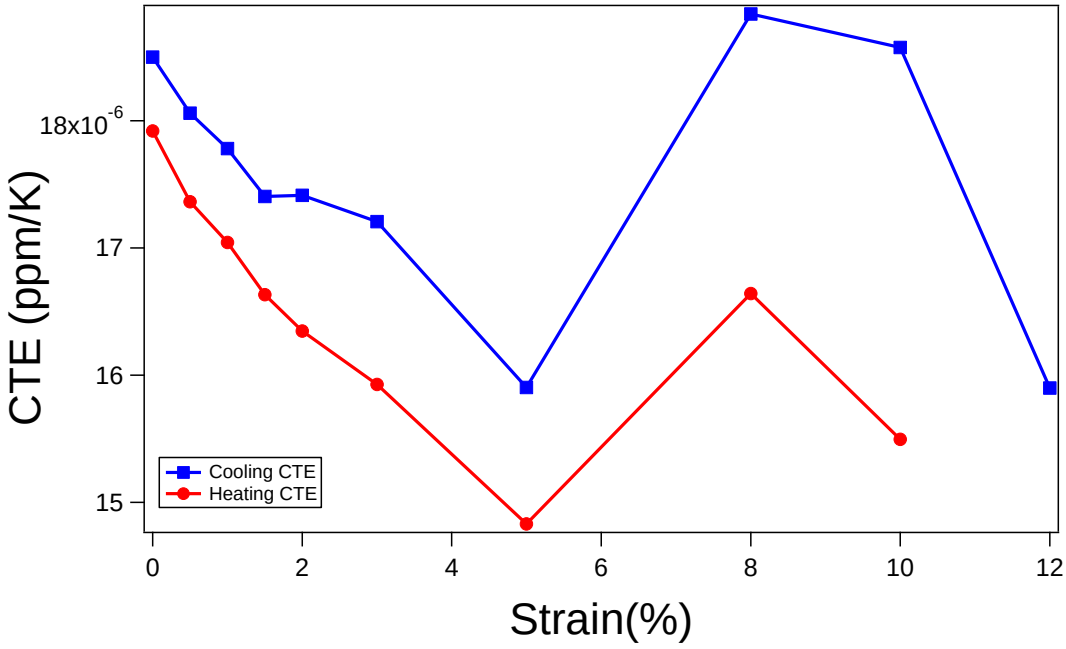

Figure 14 – CTE Response to Strain of $Cu_{68}Zn_{25}Al_7$ Heat Treated at 920°C for 30 minutes aand Quenched in an Ice Water

2.2.1.3.2. Ice Brine Quench

When a heated sample is dropped into water, the atmospheric gases that the water has absorbed gets released in the form of bubbles. This bubble formation decreases the amount of contact the water makes with the sample during quenching, slowing down the quenching rate. To help reduce this problem, salt can be added to water to create a brine. The brine mixture absorbs the atmospheric gases less, resulting in less bubble formation

and more contact between the sample and the fluid, increasing the quenching rate. A brine was used as the quenching medium for samples ,measuring 1mm thick, that were heat treated at 920ºC for 30 minutes. The results are shown in Figure 15.

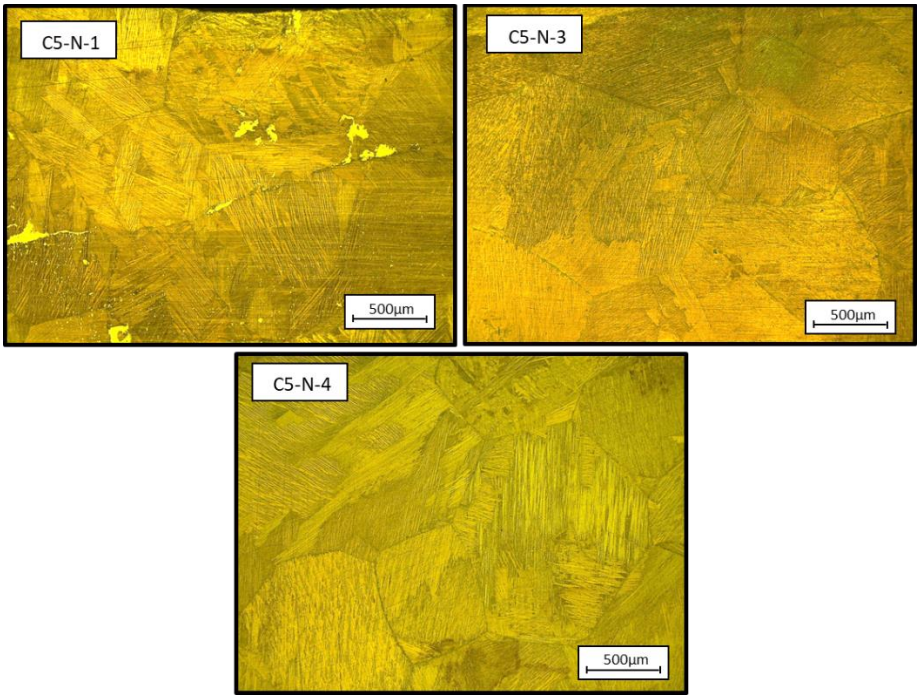

Figure 15 - Samples of $Cu_{68}Zn_{25}Al_7$ Heat Treated at 920C for 30 Minutes and Quenched in an Ice Brine

All samples show similar characteristics as previous samples with similar heat treatments: large martensitic grains. The variation between samples, from macroscopic scale, is very little, all the samples have lamellar martensite and almost no visible precipitates at the

grain boundaries. Isobaric tension tests were performed on the sample to see if the mechanical behavior between samples was the same. The results of the test, shown in Figure 16, show that three distinctively different stress strain curves. C5-N-1 has the optimal curve where martensitic reorientation occurs. C5-N-4 shows a curve similar to those in Figure 12. C5-N-3 has 23% strain, the largest strain measured from all the isothermal test performed. Macroscopically, the samples looked the same, but their mechanical behavior were all very different.

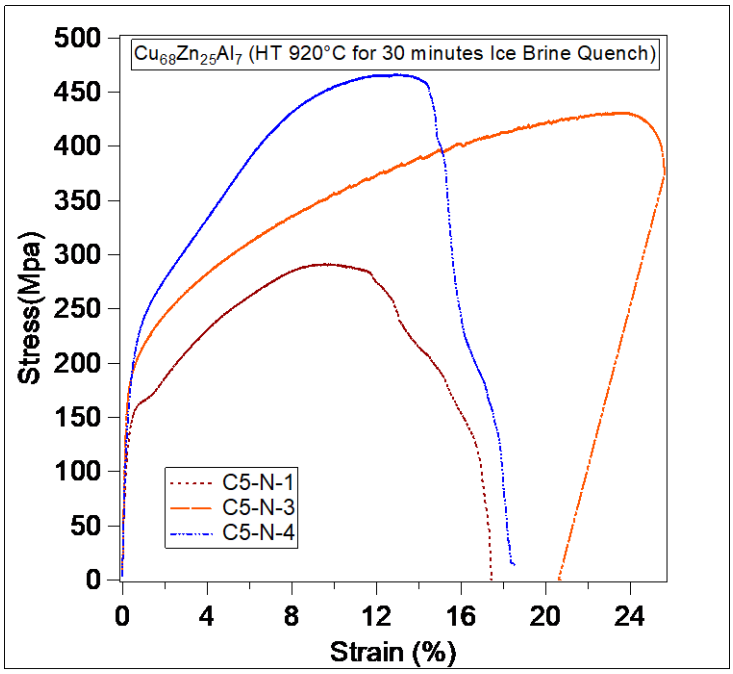

Figure 16 – Monotonic Tension Test Results of $Cu_{68}Zn_{25}Al_7$ Heat Treated at 920°C for 30 Minutes and Quenched in an Ice Brine

2.2.1.3.3. Sample Thickness Effect on Quenching Rate

The final way the quenching rate was increased was by reducing the sample thickness. Samples were cut to three different thickness: 0.50mm, 0.75mm, and 1.00mm. The samples were heat treated at 920ºC for 30 minutes and quenched in an ice brine. Four samples, two samples, and 3 samples of 0.50mm, 0.75mm, and 1.00mm thickness, respectively, were tested. The results shown in Figure 17 show a representation of the microstructure on the left and the resulting isobaric tension test on the left. Similar to previous heat treatment studies, the sample to sample variation at the macroscopic scale was very little. At 0.50mm, the grain size was the smallest, and as the sample thickness increased, so did the grain size. All samples had lamellar martensite present. The mechanical behavior varied between samples with the same thicknesses. Because of the mechanical behavior variation, there is no apparent relational between sample thickness and mechanical behavior. The only sample that showed a large amount of martensitic reorientation was the sample with 1.00mm thickness, the sample was removed in the middle of testing for further studies. Samples after Testing are shown in the Appendix.

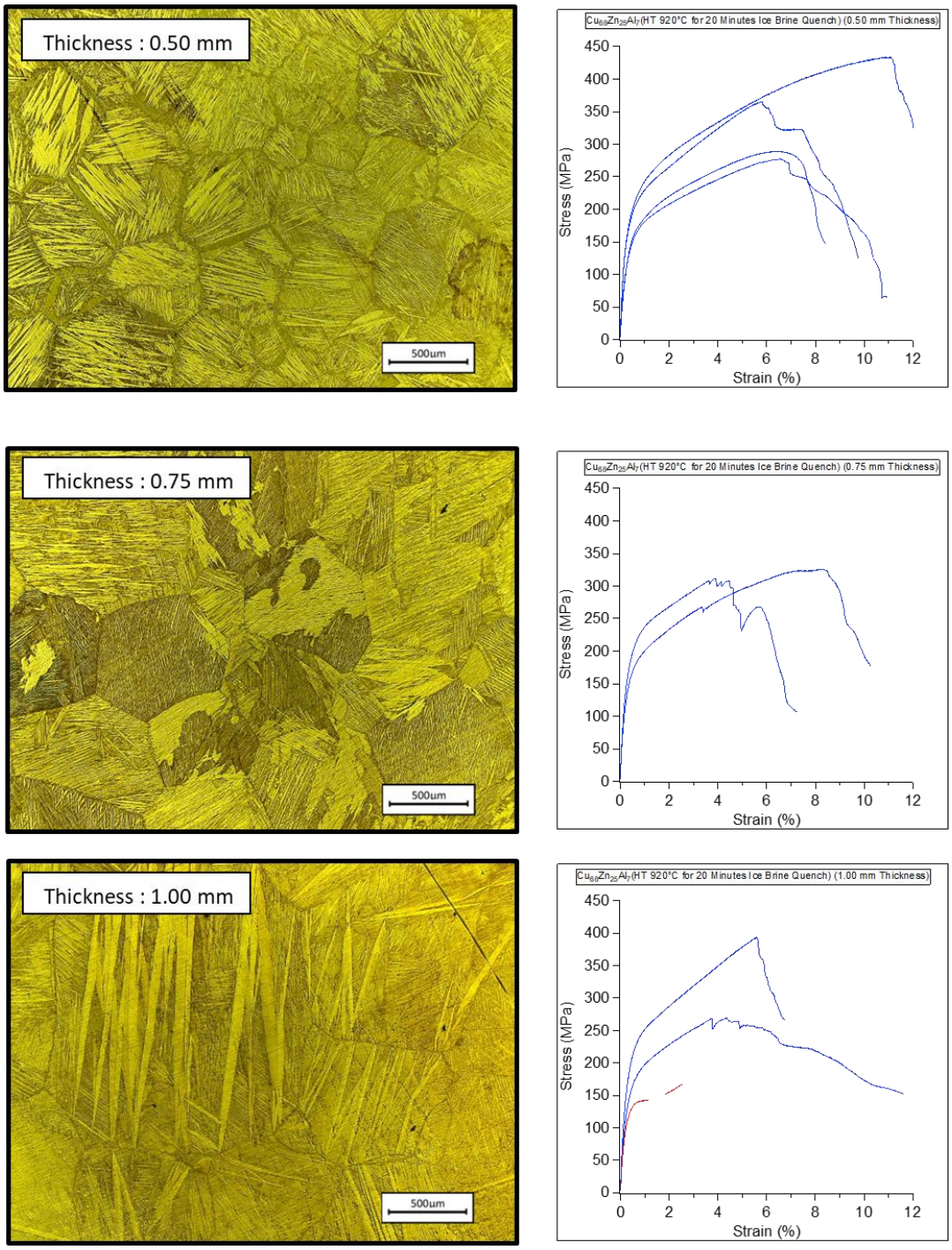

Figure 17 – Microstructure (left) and Corresponding Tension Test Results (Right) of samples of $Cu_{68}Zn_{25}Al_7$ Various Thicknesses Heat Treated at 920°C for 20 Minutes and Quenched in an Ice Brine

2.2.2. Study on $Cu_{75}Zn_{18}A_7$

2.2.2.1. Microstructural Study

Figure 18 shows the optical microscopy for a sample of as cast $Cu_{75}Zn_{18}A_7$. There is no martensite phases visible at room temperature. It is likely to be some sort of austenite phase.

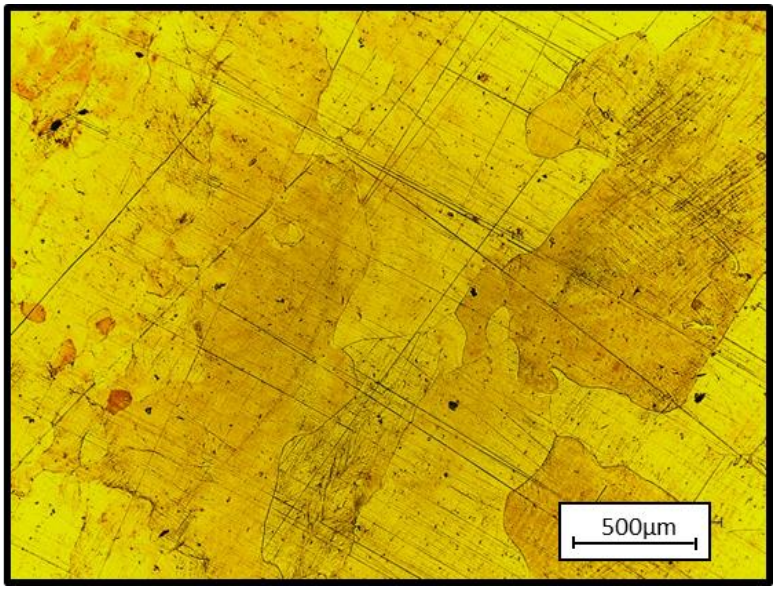

Figure 18 - Optical Microscopy for As Cast Samples of $Cu_{75}Zn_{18}A_7$

Figure 19 shows samples of $Cu_{75}Zn_{18}A_7$ microstructure after being heat treated at 630ºC, 800ºC, 850ºC, and 900ºC for 20 minutes .At temperatures at and below 800ºC, there appears to be an austenite phase and austenite twins. At temperatures above 800ºC, the

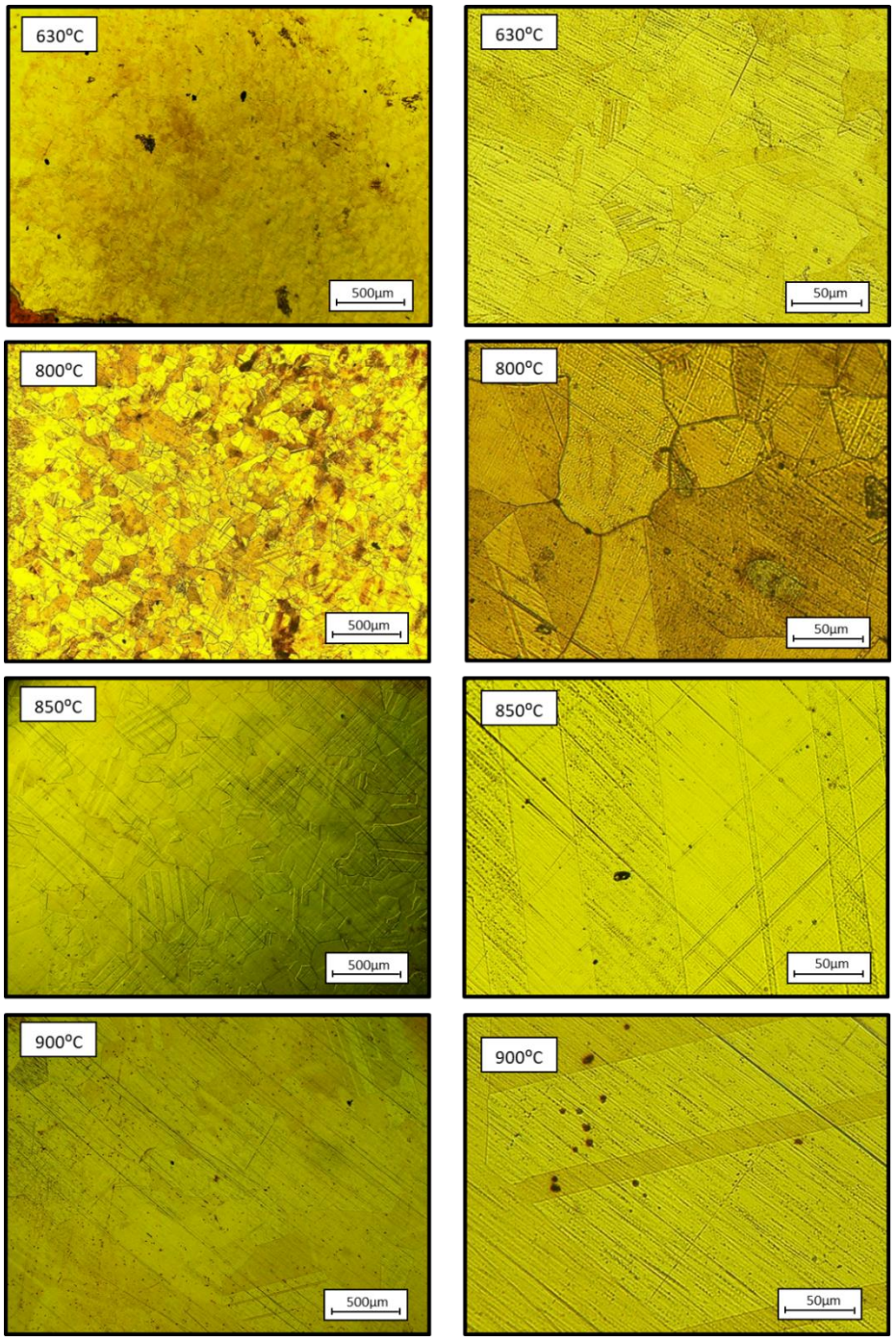

Figure 19- Heat Treatment Results of $Cu_{75}Zn_{18}A_7$ Heat Treated for 20 Minutes at Discrete Temperatures.

grain size increases the phase remains the same. Austenite is visible for all heat treatments and there is no martensite visible at room temperature. Since there is no martensite at room temperature, DSC was used to determine the transformation temperature of the sample heat treated at 800º for 20 minutes. Figure 20 shows the DSC results, The martensite start temperature is measured was determined to be about -70ºC. At these temperatures, martensite reorientation cannot be done with the equipment available. XRD was used to determine if there was any martensite and to determine if an austenite phase was present.

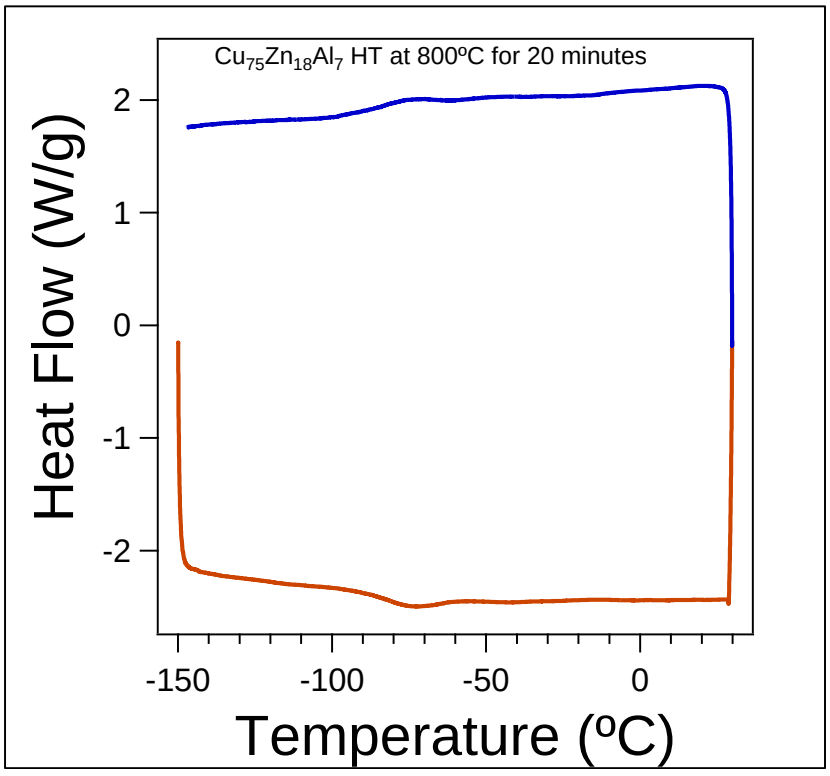

Figure 20 – DSC Results for $Cu_{75}Zn_{18}A_7$

2.2.2.2. X-Ray Diffraction Study

Figure 21 shows the XRD results for three samples heat treated for 3 hours at 800ºC, 950ºC, and 975ºC. All the samples show an austenite phase at room temperature. The samples have the same peaks with different intensities. Heated XRD scans were done on a sample heat treat at 950ºC for three hours. Figure 22 shows the results of the heated XRD scan. All the peaks shift to the left as temperature increases, showing that no NTE occurs at the atomic level. Because martensite reorientation must be performed to have tailorable CTE, no tension test was performed on this composition since martensite phase occurred at cryogenic temperatures.

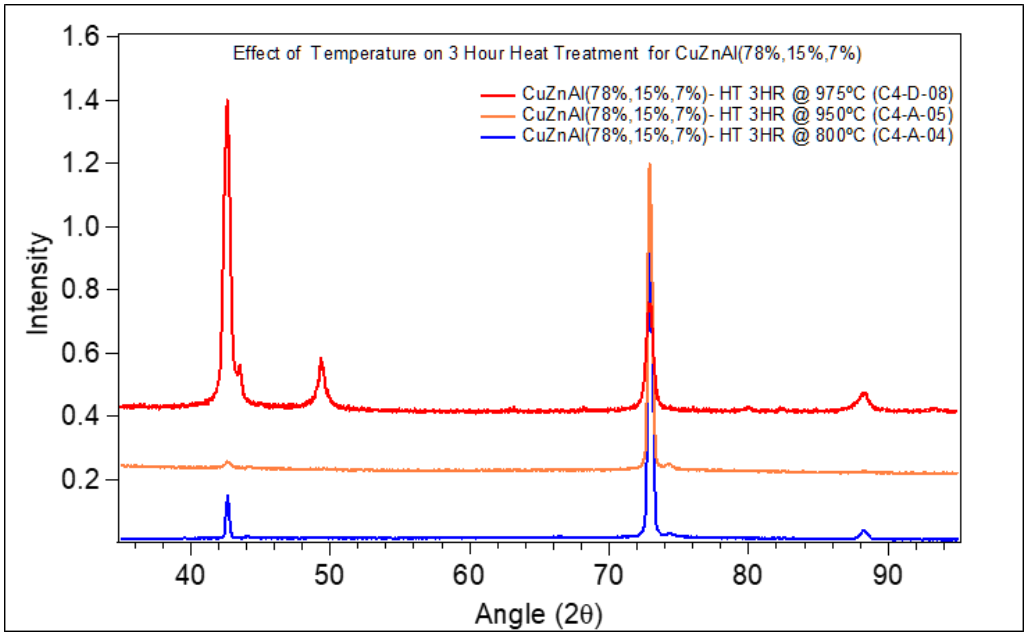

Figure 21 –XRD Results of $Cu_{75}Zn_{18}A_7$ at Different Temperatures and Times

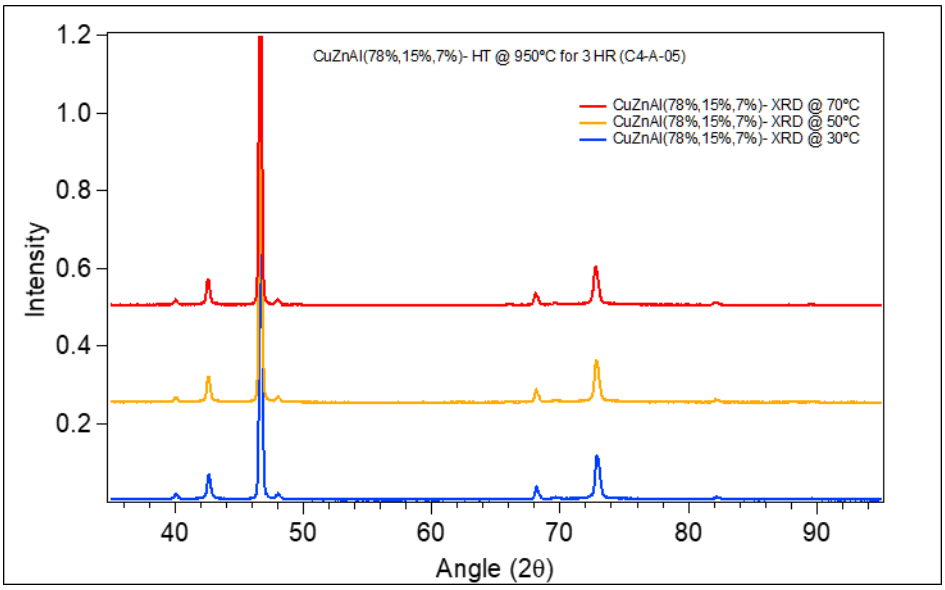

Figure 22 XRD Results for $Cu_{75}Zn_{18}A_7$ Heat Treated at 950°C for 3 Hours

.

3. INVESTIGATIONS INTO TINB

3.1. Materials and Methods

A slab of 78% and 22% (at.) of Titanium and Niobium, respectively, was casted, homogenized in Argon gas at 1200ºC, and quenched in room temperature water. Initial hardness analysis of the slab showed an α case that penetrated 2mm into the slab. The α case was removed and the slab was sectioned to process using four different methods of plastic deformation.

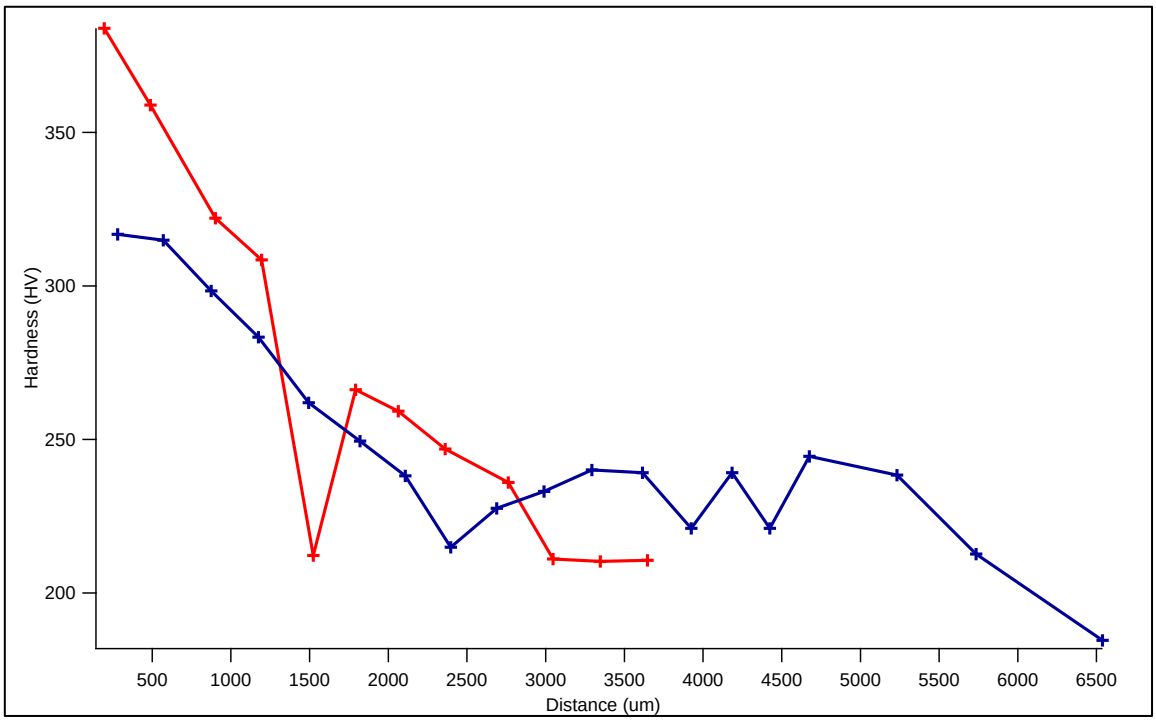

Figure 23 - Hardness Testing of the As Cast Slab Showing Penetration of the α Case

3.1.1. Deformation Methods

$Ti_{78}Nb_{22}$ rectangular bars were wire EDM with an initial thickness of 6.35 mm. The sample was rolled at room temperature with a reduction step of 0.25 mm and a constant rolling direction to 50% reduction. Samples that were backward extruded, forward estruded, and tube drawed were first cut into cylinders using wire EDM, The cylinders were then processed at room temperature to have an extrusion ration of 2. Samples measuring 25mm long were then cut using wire EDM and the CTE was calculated using sample thermal displacement data collected through the use of a dilatometer. An example of the deformation methods is shown in Figure 24

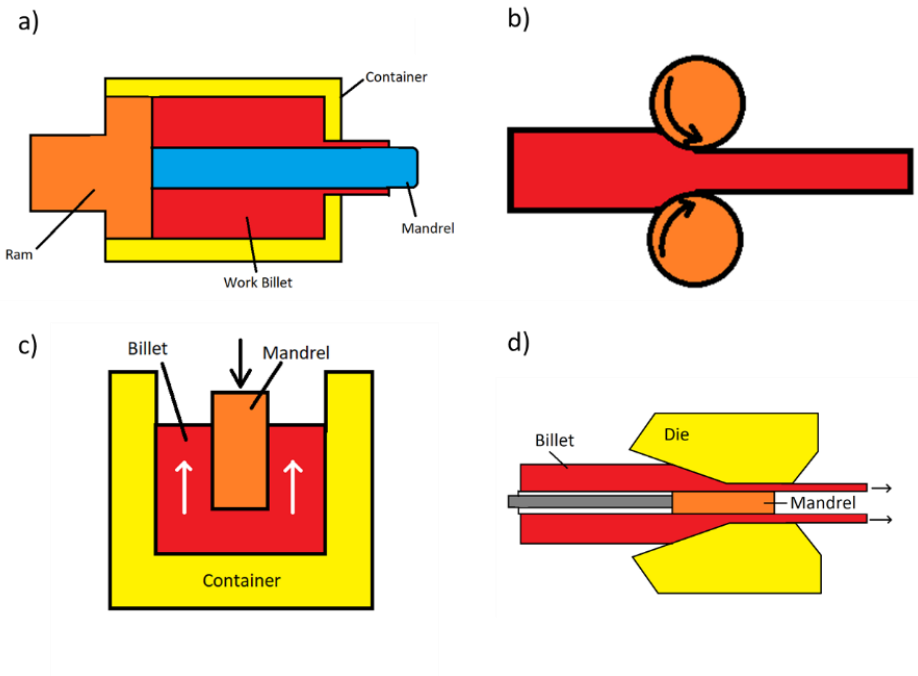

Figure 24 - Deformation Processes: a) Forward Extrusion , b) Rolling , c) Backward Extrusion , d) Tube Drawing

3.1.2. Measuring CTE

Thermal expansion testing was done using a horizontal push-rod dilatometer. The dilatometer is equipped with a copper furnace and a liquid nitrogen cooling system used to heat and cool the samples. 25mm samples were held in place with a fused silica holder, preloaded and constantly held with 0.2 N of force. The sample chamber was filled with nitrogen gas, cooled to -60ºC and ramped at 2°C/min between -60°C and 100°C. Sampled displacement was recorded and the CTE was calculated from the data.

3.1.3. CTE Tailoring Methods

3.1.3.1. Welding TiNb to Ti-6Al-4V

$Ti_{78}Nb_{22}$ was cold rolled as described previously and laser welded to Ti-6Al-4V and to another sample of cold rolled $Ti_{78}Nb_{22}$ using a seam weld and a bevel weld. Dilatometry samples were cut and the CTE was calculated using sample displacement data recorded by the dilatometer. The welded samples were also mechanical tested. Uniaxially tension test were performed at room temperature on a uniaxial MTS 312.31 Servohydraulic Test System with an MTS Load cell with a capacity of 2500lbf. Each weld sample was EDM to 25mm long tensile dogbone samples with a gauge length of 12mm. The seam welded sample had cross sectional dimensions of 3.05mm x 2.98mm. Because the bevel samples had stronger welds, the samples had to be reduced to cross sectional dimensions of 3.05mm x 1mm, with the reduction made on thickness of the width not reducing the depth of the weld. Each sample was pinned, preloaded with 10N, and clamped down to align the sample with the loading direction. A MTS extensometer (Model No. 632.53E-14) was

attached with the ceramic extension rods placed symmetrically on the sample with the center being the weld. The samples were then strain at crosshead speed of 0.004 mm/s until failure.

3.1.3.2. Relaxation Heat Treatments

A homogenized bar of $Ti_{78}Nb_{22}$ was heat treated at 600ºC for 5 hours and water quenched. This heat treatment was done to remove residual stresses caused by the homogenizing heat treatments. $Ti_{78}Nb_{22}$ was then processed using the cold rolling method described earlier. Samples measuring 25mm and 9.75 mm in length were cut using wire EDM. The dimensions of the samples were measured using a micrometer. The samples were then heat treated at different times and temperatures. The heat treatments consisted of three different temperatures and lengths of time: 200ºC, 400ºC, and 600ºC for 15 minutes, 2 hours , and 6 hours. Each heat treatment had three samples to check for variability. The sample lengths were measured again using a micrometer to calculate strain. The CTE of each sample was calculated using the thermal displacement data measured with the dilatometer.

3.2. Results and Discussion

3.2.1. Deformation Methods Results

Processed samples were tested in a dilatometry and the CTE was calculated. The results are shown in Figure 25. Different processing methods resulted in different values of CTE. Backward extrusion and cold rolling resulted in very similar CTE curves. Forward

extrusion had the second largest negative CTE value. Tube drawing resulted in the largest negative CTE. The results were curved fitted to calculate values at room temperature tabulated in Table 5.

Previous studies in NTE showed that the relationship between strain and CTE was not linear. At some point, increasing strain had negligible effect on the CTE. The results showed that larger negative CTE values can be acquired by using different processing methods. Having more options in CTE values and shapes increases the applicability of the material. Keeping the samples straight while cold rolling became increasingly difficult as the thickness of the samples were increased. This limited the final thickness of bars to be no greater than 4mm. Long lengths of both forward and backward extruded samples were difficult to produce because of the large forces required to deform the sample at room temperature. Extrusion methods created large amounts of unusable material that could not be extruded . Tube drawing was the most effective method of achiving NTE. It produces the least amount of waste material compared to extrusion methods, the largest negative CTE of all methods, and the long lengths of tubes can be drawn much easier than through extrusion.

Table 5 CTE Results of Different Processing Methods at Room Temperature

Processing Method	Maximum CTE at RT (ppm/K)
Rolling	-19.86
Back Extrusion	-20
Forward Extrusion	-25.082
Round Bar	-31.2

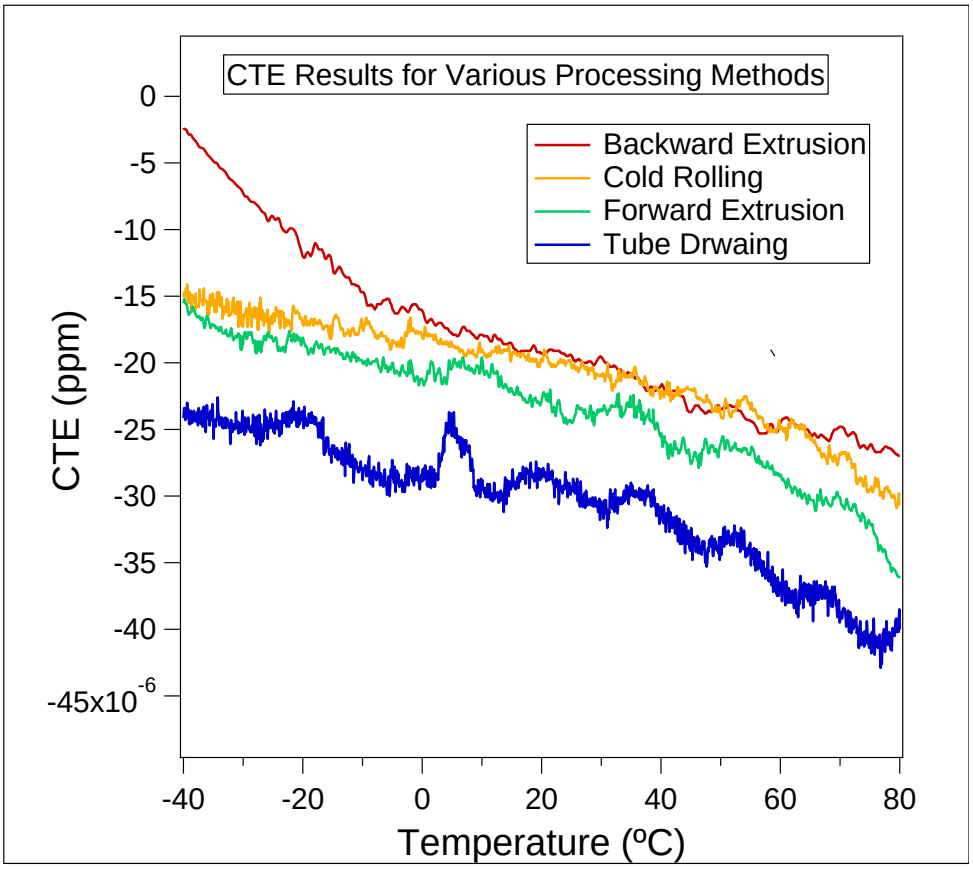

Figure 25 – Dilatometry Results of Different Processing Methods

3.2.2. Welding $Ti_{78}Nb_{22}$ to Ti-6Al-4V

3.2.2.1. CTE Results

Figure 26 shows the microstructure of Ti-6Al-4V seam and bevel welded to $Ti_{78}Nb_{22}$ along with two samples of $Ti_{78}Nb_{22}$ bevel welded to each other using a Ti-6Al-4V rod. The contrast in the materials shown in the x-ray spectroscopy images allow the Ti-6Al-4V and $Ti_{78}Nb_{22}$ to be differentiated. The melt pool shows both materials present, indicating that $Ti_{78}Nb_{22}$ and Ti-6Al-4V are miscible.

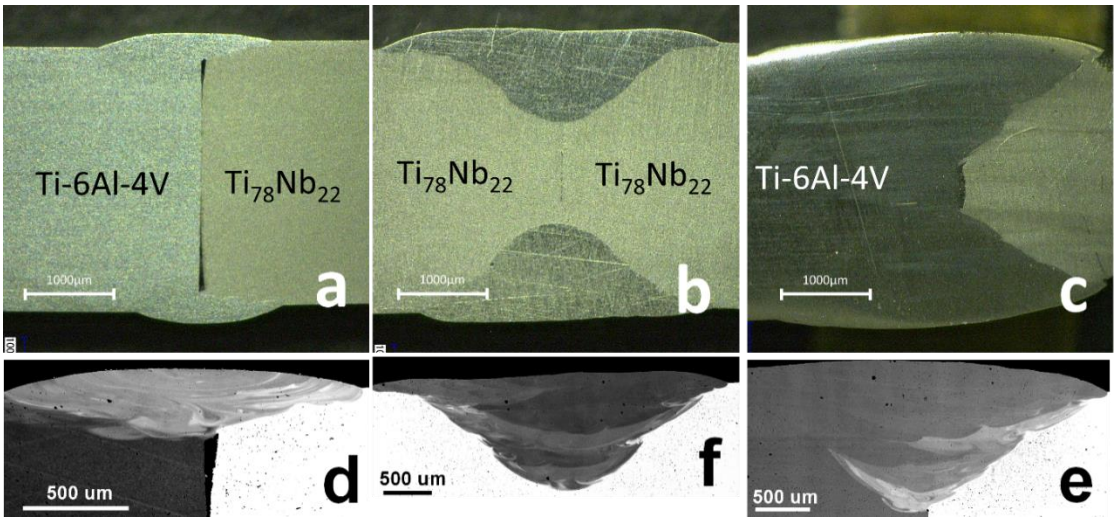

Figure 26- a) $Ti_{78}Nb_{22}$ seam welded to Ti-6Al-4V b) $Ti_{78}Nb_{22}$ welded to $Ti_{78}Nb_{22}$ c) $Ti_{78}Nb_{22}$ bevel welded to Ti-6Al-4V and Their Respective X-Ray Images below

High miscibility is needed to create strong bonding when joining materials. Welding is an excellent way of joining metals together, but the high heat required can create heat affected zones. In SMAs, heat can raise the temperature of the material and cause a phase

transformation. This can affect the NTE of the material because the NTE is related to the martensite and austenite structures. NTE only occurs in the martensite phase, and the heat affected zones can lose their martensite phase. By combining materials with different CTE, the CTE of the combined material can be altered. To study the effects of joining materials, the CTE was calculated using data from dilatometry results.

The CTE calculated is shown in Figure 27. The CTE of the $Ti_{78}Nb_{22}$ bevel welded to $Ti_{78}Nb_{22}$ has a similar curve to the $Ti_{78}Nb_{22}$ sample and the CTE changed slightly. The $Ti_{78}Nb_{22}$ welded to Ti-6Al-4V samples have a CTE that is a combination of the $Ti_{78}Nb_{22}$ and Ti-6Al-4V. They are also relatively stable when compared to the $Ti_{78}Nb_{22}$ samples.

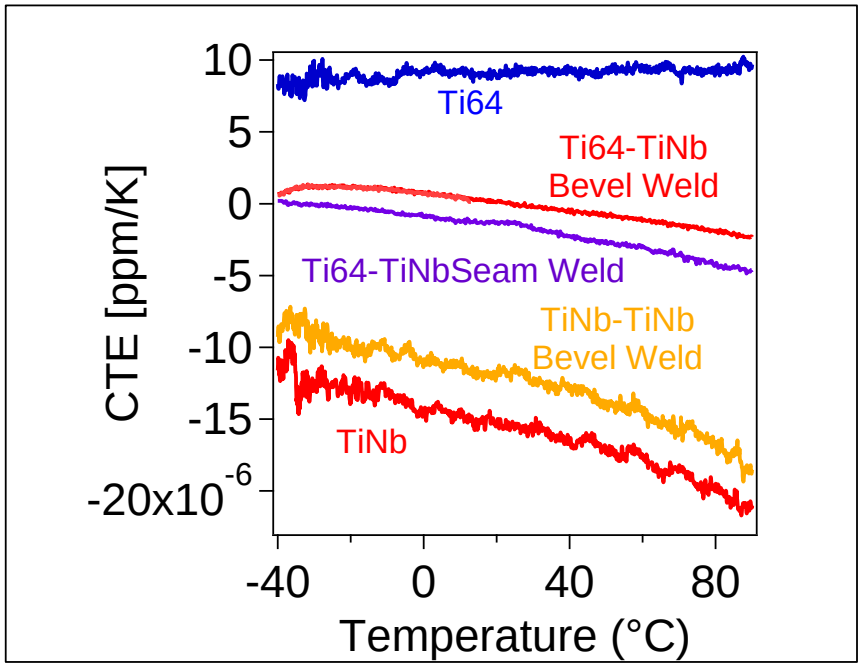

Figure 27- CTE vs Temperature of (Listed from top to Bottom) Ti-6Al-4V, Ti-6Al-4V Bevel Welded to $Ti_{78}Nb_{22}$, Ti-6Al-4V Seam Welded to $Ti_{78}Nb_{22}$, $Ti_{78}Nb_{22}$ Bevel Welded to $Ti_{78}Nb_{22}$, and $Ti_{78}Nb$

Figure 28 shows the CTE at 20°C of the welded samples and pure samples. The samples CTE follow the rule of mixtures. Using the rule of mixtures, the CTE can be tailored by changing the percentage of each material in a composite. The welded samples lay above the rule of mixtures predicted results, this is because of the heat affected zones. The bevel welds create larger heat affected zones than the seam weld which is why the bevel welds lie further away from the predicted results.

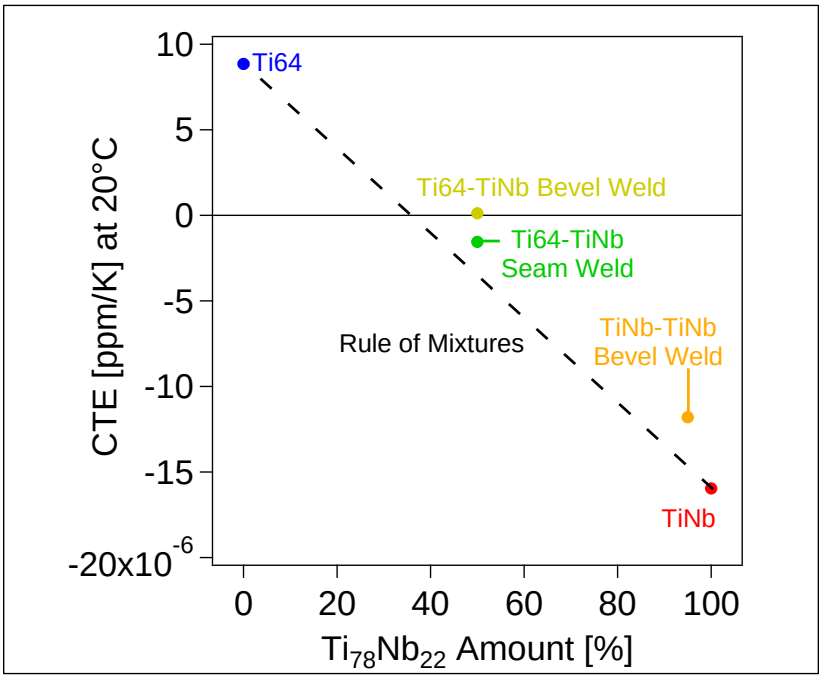

Figure 28- Rule of Mixtures and Welded Samples CTE

3.2.2.2. Mechanical Testing

Figure 29 shows the stress-strain response for uniaxial tensile testing from welded and non-welded samples. $Ti_{78}Nb_{22}$ annealed refers to the unprocessed material. The yield strength was determined using the 0.2% offset method. A summary of the results is shown in Table 6. Because the welded samples have sections where the two materials are not joined, two different cross-sectional areas were used to determine the strengths of the materials, the cross-sectional area of the weld and the cross-sectional area of a uniform

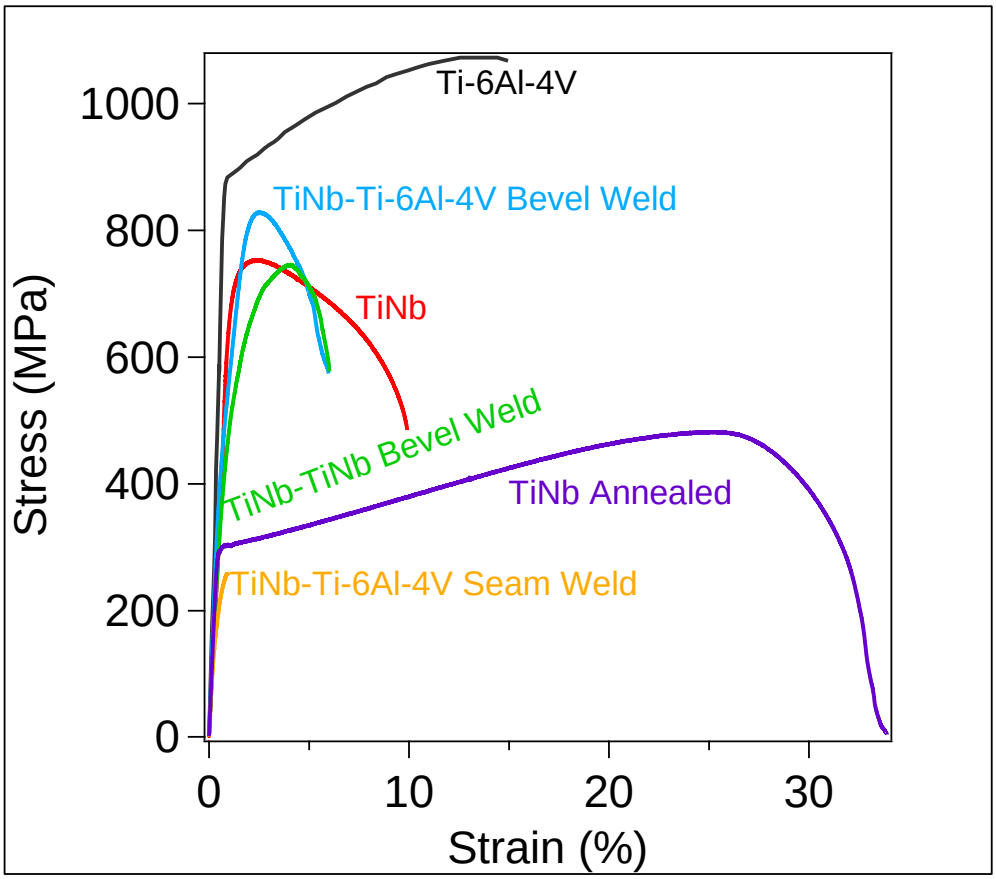

Figure 29 – Tension Test Results of Welded Samples

section of sample. The adjusted strengths correspond to the cross-sectional area of the weld and the unadjusted strengths correspond to the cross-sectional area of a uniform section of the sample.

Table 6 Mechanical Properties of the Welded Samples

Sample	Yield Strength [MPa]	Adjusted Yield Strength [MPa]	UTS [MPa]	Adjusted UTS [MPa]
Ti-6Al-4V	883	-	1072	-
$Ti_{78}Nb_{22}$	723	-	752	-
$Ti_{78}Nb_{22}$ Annealed	297	-	482	-
$Ti_{78}Nb_{22}$-ALLVAR Bevel Weld		**660**	746	**1069**
$Ti_{78}Nb_{22}$- Ti-6Al-4V Bevel Weld	487	**553**	828	**973**
$Ti_{78}Nb_{22}$- Ti-6Al-4V Seam Weld	209	**891**	256	**1212**

Because of the non-uniformity of the welded samples, the shape of the curve does not follow the typical shape of uniform materials. Different materials begin to yield at different amounts of strain, causing an undefined yield point. The yield strength for the welded samples was measured using the 0.2% offset method, where the linear section starting from 0% strain was used as the slope to indicate the yield strength. Both adjusted and unadjusted yield strengths of the bevel welded samples are between the yield strength of $Ti_{78}Nb_{22}$ and annealed $Ti_{78}Nb_{22}$. The unadjusted yield strength of the seam welded sample is lowest of all samples. The adjusted yield strength of the seam welded sample is

the highest of all samples and very similar to that of Ti-6Al-4V. Sample after Testing are shown in the Appendix.

The ultimate tensile strength for the bevel welded samples describe the strength of the material used for the cross-sectional area. In all welded samples, the $Ti_{78}Nb_{22}$ section will fail before the Titanium-64 section and weld fails. When using the cross-sectional area of a uniform section of the sample, the UTS is similar to the UTS of the $Ti_{78}Nb_{22}$. When the cross-sectional area of the Ti-6Al-4V weld is used, the UTS is similar to that of Ti-6Al-4V. This fact is true for the seam welded sample. The unadjusted UTS of the seam weld is the least of all samples.

All welded samples fail before $Ti_{78}Nb_{22}$, Ti-6Al-4V, and annealed $Ti_{78}Nb_{22}$ do. The bevel weld samples both fail at about 6% strain. The seam welded sample failed at the lowest strain of 0.9% strain.$Ti_{78}Nb_{22}$ welded Ti-6Al-4V produce a composite that has good mechanical properties and CTE coefficients that can be tailored to an extent. The miscibility between $Ti_{78}Nb_{22}$ and Ti-6Al-4V allow parts to be joined together when used in application.

3.2.2.3. Post Heat Treating Processed Samples Results

Another way to alter the CTE of processed $Ti_{78}Nb_{22}$ is decreasing the amount of oriented martensite. Rolled samples of $Ti_{78}Nb_{22}$ were post heat treated at 200°C, 400°C, and 600°C for 15 minutes, two hours and six hours. The temperatures were chosen based on phases

transformation that occur at these temperatures. At 200°C, $Ti_{78}Nb_{22}$ is above it A_f temperature and near the temperature meta-stable ω phase precipitates begin to form. By going into this temperature regions, some remnant austenite may not transform when the temperature is below M_f temperature, thus reducing the amount of martensite present. At 400°C, ω precipitates are present. In this region, ω phase precipitates are expected to appear and grow. By heat treating at this temperature, the amount of austenite that will transform to martensite is reduced. At 600°C, recrystallization is expected to occur, completely removing any grain orientation present in the material. When the sample is returned to room temperature, it is expected that new martensite variants will be present and the would be no orientation.

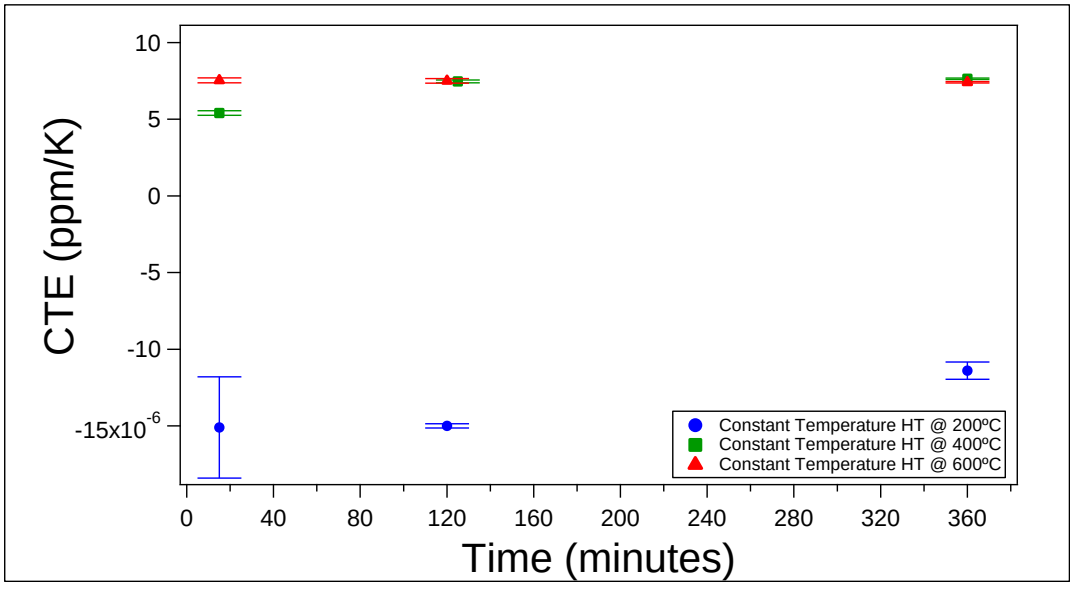

Figure 30- Length of Time of Effects on CTE for Multiple Heat Treatments

Figure 30 shows CTE as a function of the time for three different heat treatment temperatures. At 200°C, the CTE increase slightly, but remains negative after being heat treated for 6 hours. For heat treatments at 400°C and 600°C, the CTE turns positive immediately at after being heat treated for 15 minutes. At 400°C, the CTE is positive, but lower than the CTE of samples that were heat treated longer. At 600°C, there is no orientation remaining and the CTE remains the same for all lengths of times.

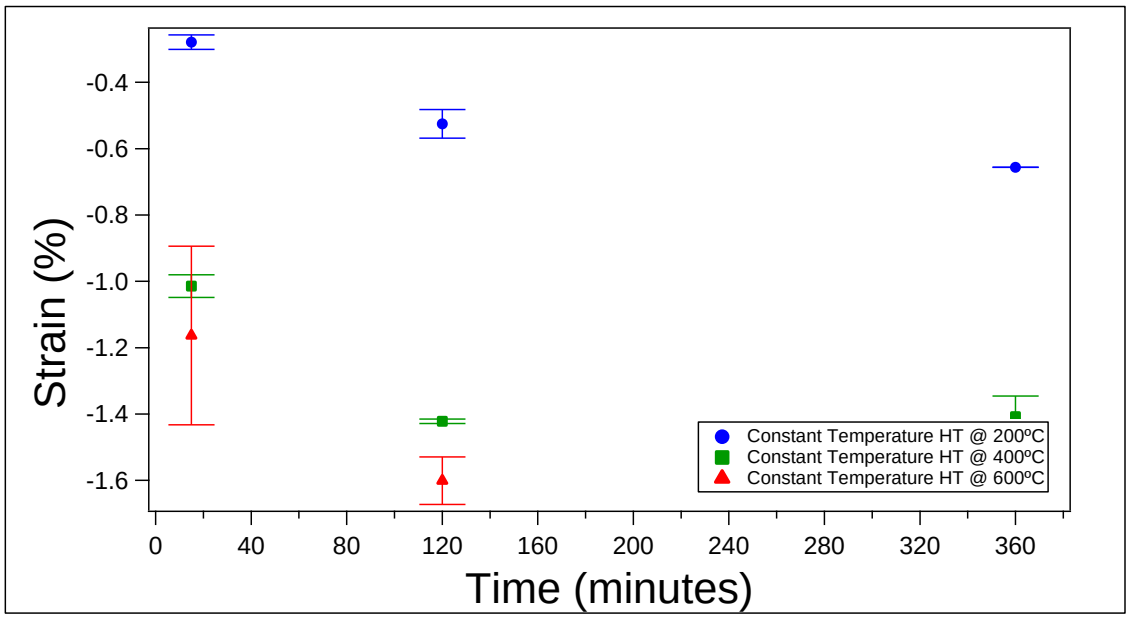

Figure 31 - Length of Time of Effects on Strain for Multiple Heat Treatments

Figure 31 shows the amount of strain measured as a function of time of the heat treatments. Higher temperatures increased the strain for every length of time the samples were heat treated. The amount of strain continued to increase at 200°C as the heat treatment time

increased. For 400°C and 600°C heat treatments, the amount of strain increased after 15 minutes, but did not change after being heat treated for 2 hours and 6 hours. The strain for all temperatures were always greater than the strain caused by lower temperatures for all lengths of times.

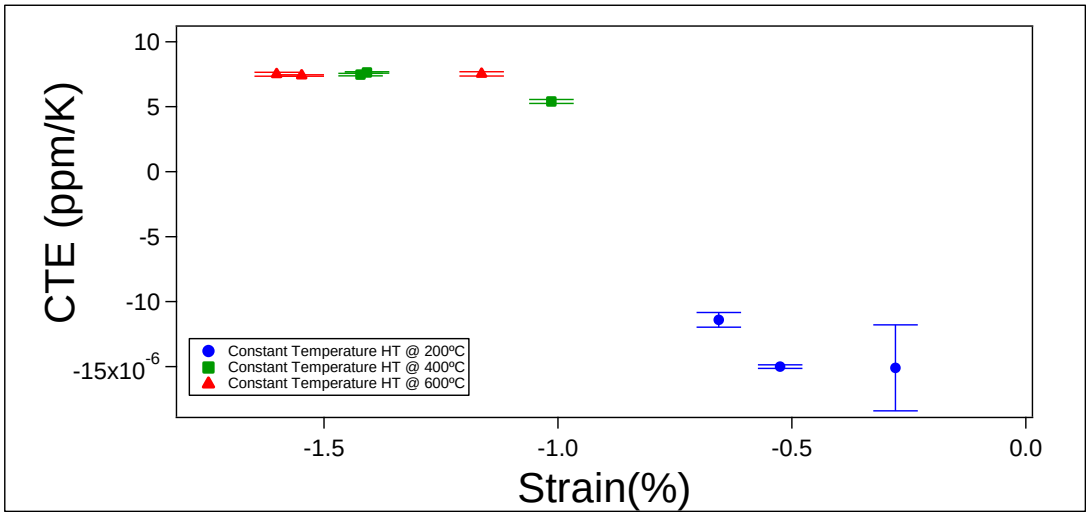

Figure 32 Length of Time of Effects on CTE for Multiple Heat Treatments

Figure 32 shows the CTE as a function of strain. The relationship between strain and CTE is not linear, it follows an S curve. After -1% strain, the CTE does not change. The results show as the samples lose their orientation, the sample length decreases, this decreasing the amount of negative CTE. At some point strain does not affect the CTE of the samples. By post heat treating processed samples, the CTE can be tailored. Different temperature

and time combination need to be done to complete the S curve and the samples need to be cycled to determine if the CTE is stable.

4. CONCLUSIONS

4.1. Conclusions on CuZnAl

Two compositions of CuZnAl were tested to see if they had NTE expansion and if their CTE could be tailored. Through XRD analysis and mechanical testing, it was determined that $Cu_{68}Zn_{25}Al_7$ does not have NTE. However, it was determined that the CTE can be tailored to an extent, by reorienting the martensite. This experiment has also shown that $Cu_{68}Zn_{25}Al_7$ would not be a good option for applicational use. One limitation is the thickness of the product. Heat treatments studies showed that the thickness of the sample affects the cooling rate and the microstructure, to have a consistent microstructure, the $Cu_{68}Zn_{25}Al_7$ must remain thin. Another limitation is the sample to sample variation. Although the microstructure might look the same, the mechanical properties can vary dramatically. This inconsistency make $Cu_{68}Zn_{25}Al_7$ very difficult to be applied to applications that require repeatability and precision.

$Cu_{75}Zn_{18}Al_7$ was determined to have a transformation temperature that are too low to be tested. The low transformation temperatures may make it applicable towards cryogenic uses, but not for optical uses.

4.2. Conclusions on TiNb

$Ti_{78}Nb_{22}$ is an excellent candidate for applicational uses. It can be processed using many methods to produce NTE. The best method is round drawing, as it produced the lowest

NTE and also the longest tubes. Tubes and round bars are highly applicable to many products as tubes can be formed into a variety of things, such as : fasteners, rings, structural and components.

$Ti_{78}Nb_{22}$ can also be welded successfully to Ti-6Al-4V. By welding $Ti_{78}Nb_{22}$ to Ti-6Al-4V, the CTE can be predicted using the rule of mixtures. Because Ti-6Al-4V has a stable CTE, welding it to $Ti_{78}Nb_{22}$ increases the composite's CTE over a range of temperatures. By changing the percentage of each material, the CTE can be tailored. The mechanical properties of the welds are also very good. The yield strengths and UTS are very similar to $Ti_{78}Nb_{22}$ and Ti-6Al-4V, making welding a viable option to joining these two metals. Tailoring the CTE by post heat treating processed metals is also possible. By introducing different phases, the amount of oriented martensite can be decreased by using a combination of different time and temperature heat treatments.

REFERENCES

i Patoor, E., Lagoudas, D., Entchev, P., Brinson, L. and Gao, X. (2006). Shape memory alloys, Part I: General properties and modeling of single crystals. *Mechanics of Materials*, 38(5-6), pp.391-429.

ii Otsuka, K. and Wayman, C. (2002). Shape memory materials. Cambridge: Cambridge University Press.

iii Otsuka, K. and Wayman, C. (2002). Shape memory materials. Cambridge: Cambridge University Press.

iv Otsuka, K. and Wayman, C. (2002). Shape memory materials. Cambridge: Cambridge University Press.

v Ma, J., Karaman, I. and Noebe, R. (2010). High temperature shape memory alloys. International Materials Reviews, 55(5), pp.257-315.

APPENDIX

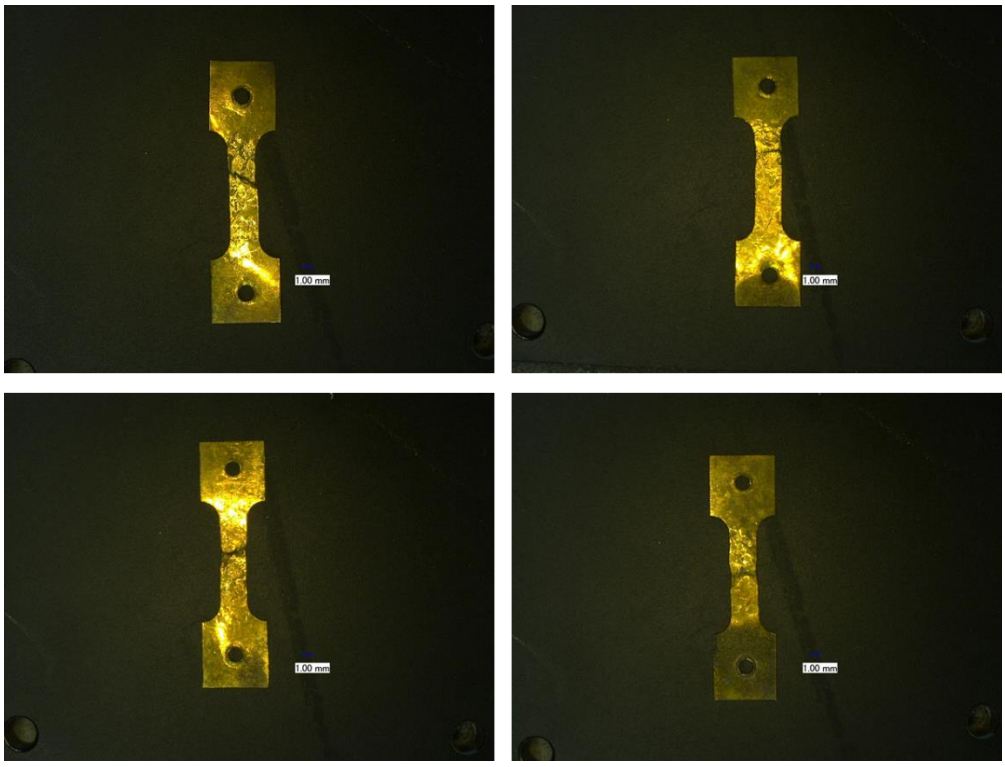

Figure 33 - 0.50 mm Samples After Tension test

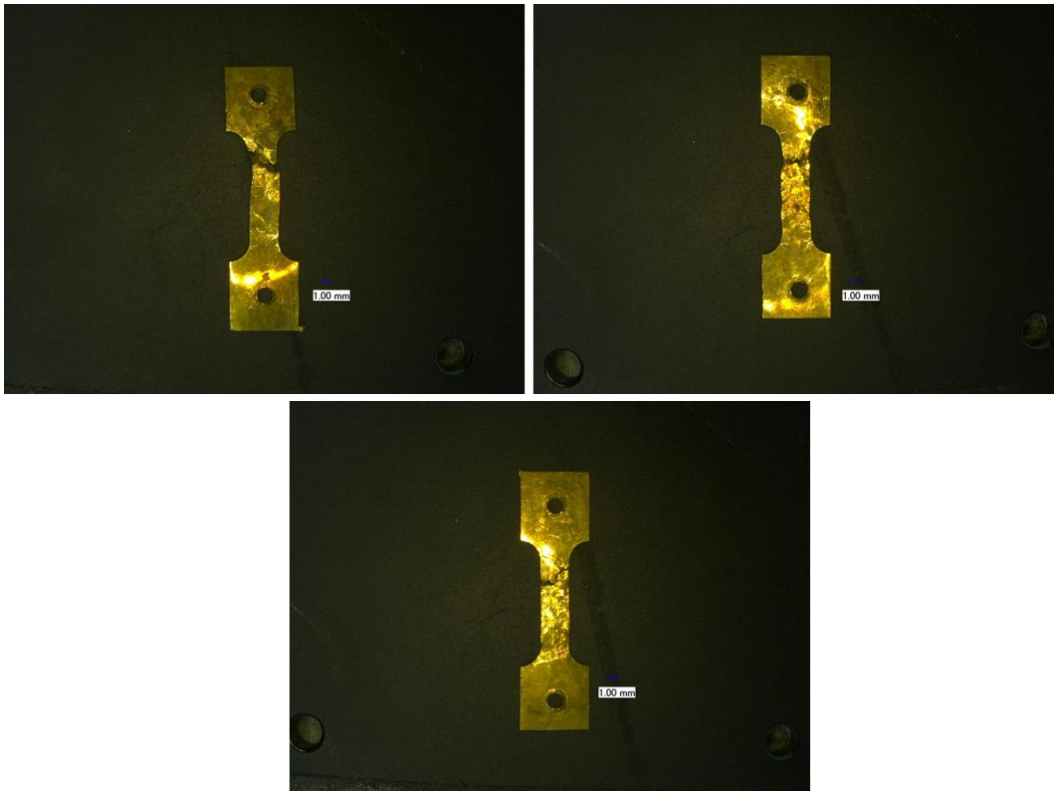

Figure 34- 0.75mm Samples After Tension Test

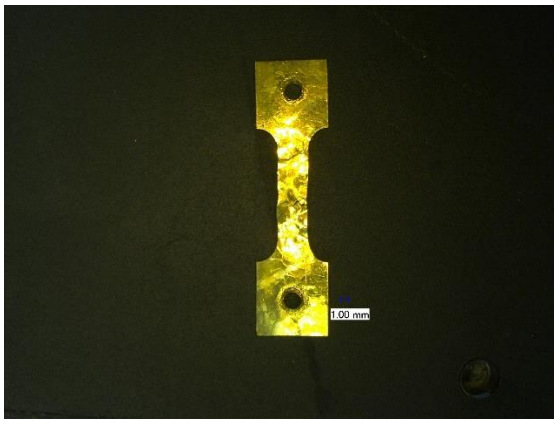

Figure 35- 1mm Sample After Tension Test

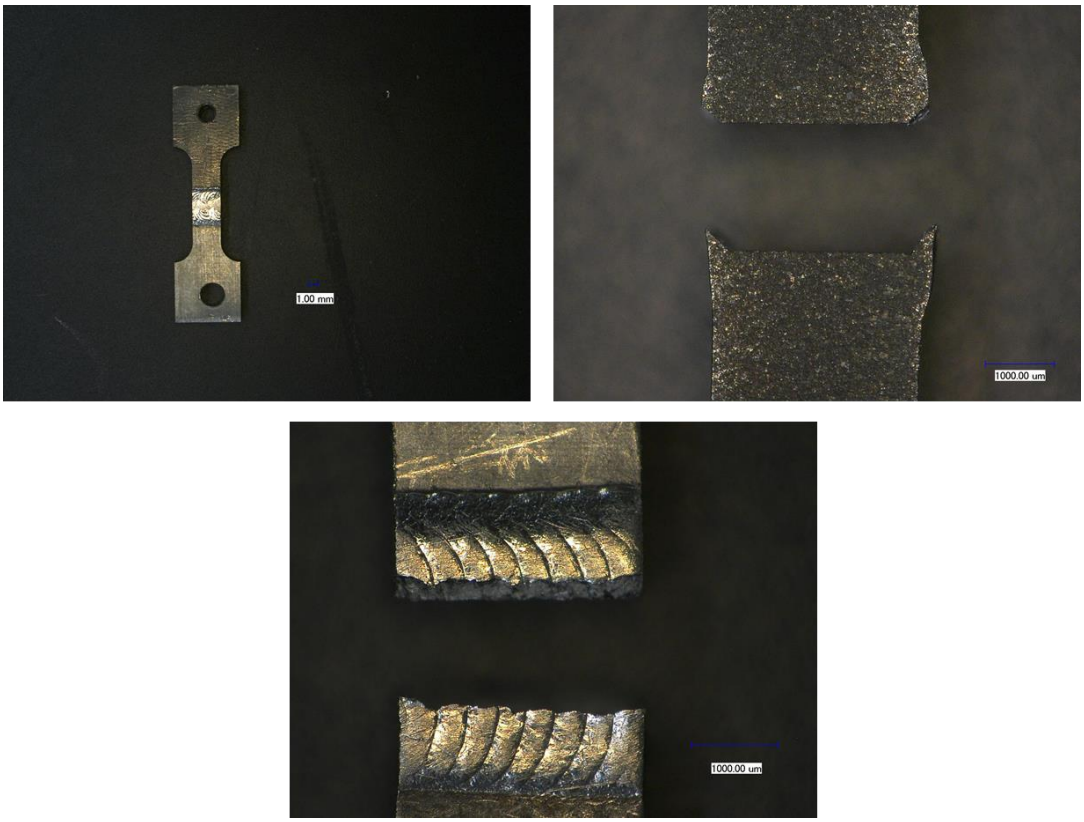

Figure 36- Seam Welded Sample Before and After Tension Test

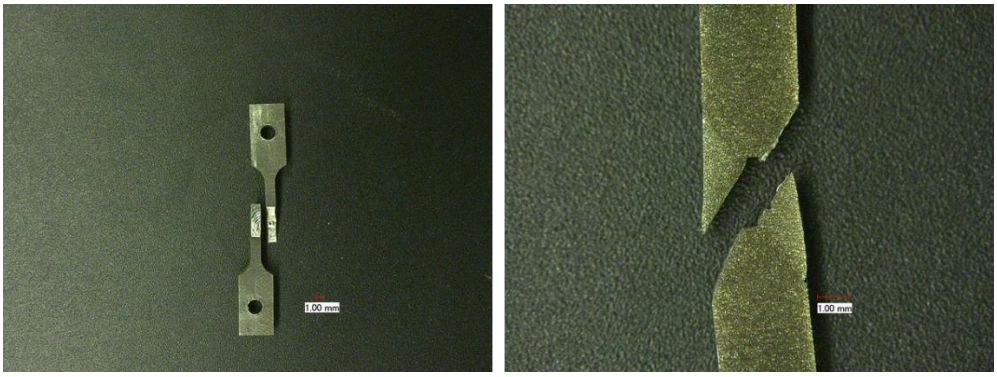

Figure 37-TiNb to TiNb Welded Sample After Tension Test

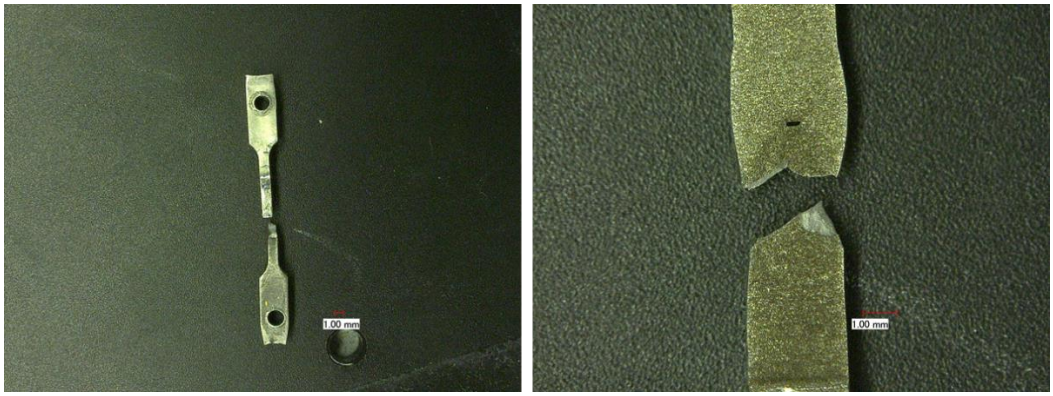

Figure 38- Ti-6Al-4V Bevel Welded To TiNb After Tension Test